

Aus der Klinik für Augenheilkunde der Universität zu Lübeck

Direktor: Prof. Dr. med. Salvatore Grisanti

**Tanshinone IIA and Apigenin as Potential and
Natural Inhibitors of the Metastatic Activities of
Uveal Melanoma Cells**

INAUGURALDISSERTATION

zur

Erlangung der Doktorwürde

der

Universität zu Lübeck

-aus der Sektion Medizin-

vorgelegt von

Huaxin Zuo

aus Heilongjiang, China

Lübeck 2018

1.Berichterstatter: Prof. Dr. med. Salvatore Grisanti

2.Berichterstatter: Priv.-Doz. Dr. med. Patrick Terheyden, MA

Tag der mündlichen Prüfung: 23.11.2018

zum Druck genehmigt. Lübeck, den 23.11.2018

-Promotionskommission der Sektion Medizin-

INTRODUCTION	1
1. Anatomy and histopathology	1
2. Clinical presentation and risk factors	2
3. Existing approaches of UM treatment and corresponding limits	3
3.1 Local treatments.....	4
3.1.1 Transpupillary thermotherapy (TTT).....	4
3.1.2 Radiotherapy.....	5
3.1.3 Surgical resection.....	6
3.2 Treatment of metastatic disease.....	6
4. Pathogenesis	8
4.1 Rho/ Rho-kinase/ YAP signaling pathway underlying the GNA-driven UM development.....	8
4.2 Synthetic Rho-kinase inhibitors to suppress the pathological Rho-kinase activity in UM.....	10
5. Phytochemical therapy	12
5.1 Flavonoids and their promising bioactive properties	13
5.2 Tanshinone IIA.....	16
5.3 Apigenin.....	17
6. Research purpose	18
METHODS	20
RESULTS	32
DISCUSSION	46
SUMMARY	60
Zusammenfassung	61
REFERENCES	64
APPENDIX	78
1. Abbreviations	78
2. Materials	82
ACKNOWLEDGEMENT	88
CURRICULUM VITAE	89

INTRODUCTION

Uveal melanoma (UM) is the most common primary intraocular malignant tumor in adults aged 50-60 years old, who have no known family history. The disease commonly affects a unilateral eye. UM accounts for approximately 5% to 6% of all primary melanomas and about 85% to 95% of the ocular melanoma cases. The annual incidence rate is approximately 5.3~8.6 cases per million people (7,105). Though white people share a higher prevalence of UM than other racial groups, its incidence rate in China (approximately 0.37 per million) is only second to retinoblastoma (which is most frequently found in children) (41,52).

Nowadays, the diagnosis and treatment of primary UM are not the major problem. Over 90% of the local tumors can be controlled with the radioactive plaque brachytherapy (23). However, all-cause mortality rates were 49.0% at 15 years and melanoma-related mortality rates after irradiation were 24.6% within 15 years (77). This is due to the metastasis of the primary UM mainly in the liver (89%) and lung (29%) (21,44) via the bloodstream and rarely through direct dissemination to nearby tissues. So far, no therapeutic measures were proven to be effective in preventing the metastatic activities of UM cells and further improving the survival rate.

Unlike cutaneous melanoma, UM is triggered by mutations in the GNAQ or GNA11 genes encoding the G-protein alpha-subunits Galpha-q and Galpha-11, respectively, which lead to the conversion of these signaling proteins into a constitutively active form (99). However, the precise molecular mechanisms

underlying the GNA-driven UM development still remain to be elucidated. Recent studies found that an increased activity of the transcriptional coactivator Yes-associated protein (YAP) downstream of the Rho/Rho-kinase signaling pathway is related to the growth of UM cells with Galpha-q/11 mutations (112,24). The Rho/Rho-kinase pathway is an important regulator of actin cytoskeleton organization, and implicated in numerous aspects underlying cancer progression, including proliferation, migration, adhesion, matrix remodelling, angiogenesis, and gene expression (102). Several synthetic Rho-kinase inhibitors were reported to interfere with the cytoactivity and survival of UM cells *in-vitro*. However, the research on this subject is limited and the novel Rho-kinase inhibitors would require a long process of evaluation before receiving approval in the clinical application.

As one of the most widely distributed natural metabolites of plants and fungi, flavonoids have demonstrated many potential bioactive functions, such as the suppression of metastatic activities of various tumor cells by interfering with cellular events that are mainly regulated by Rho-kinase. More excitingly, certain flavonoids have been clinically utilized for cardiovascular diseases and highly recommended as routine nutritious supplements. However, there is no study so far aiming at the possible effects of flavonoids on UM cells. Accordingly, our work specifically focused on the potential of the flavonoids tanshinone IIA and apigenin for suppressing the metastatic activities of UM cells and aimed to determine whether the Rho/Rho-kinase signaling pathway is involved in the underlying mechanism.

1. Anatomy and histopathology

UMs are melanocytic neoplasms that are generally found in the iris (3-5%), ciliary body (5-8%) and choroid (~85%). These three parts make up the uveal tract, which form the deeply pigmented vascular middle layer of the eye. (Figure 1A) Historically, UM is divided into three histological classifications: spindle, epithelioid (over 75%), and mix cellularity. Spindle cells are characterized by fusiform morphology arranged in bundles with non-typical intermediate junctions. In contrast, epithelioid cells present with big foam-like, oval-shape with more frequent mitotic figures in the nucleus. (Figure 1B, 1C) Spindle cells are regarded as a better differentiated UM type with less metastatic potential compared to the epithelioid cells. This might be partially because of the non-typical intermediate cell-cell junctions and filamentous or finger-like protrusions on cell surface, which might help strengthen the cellular connections and inhibit metastasis (8).

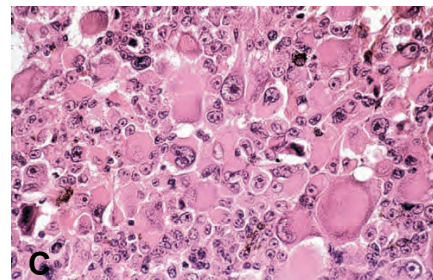
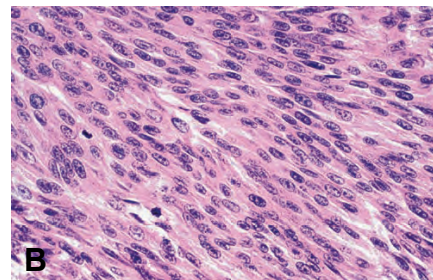
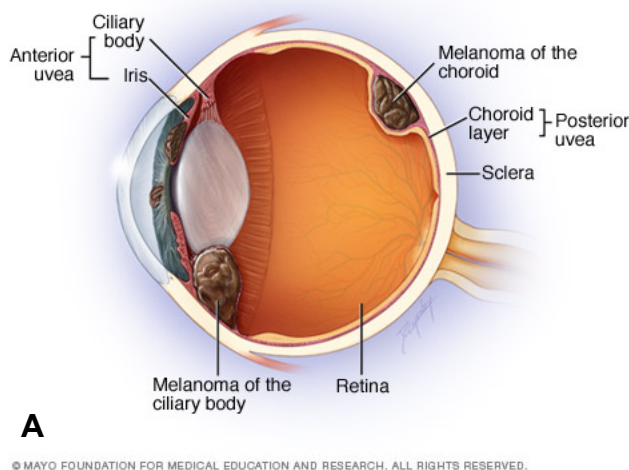


Figure 1. A. Anatomy of the three typical sites of UM: iris, ciliary body and choroid. * B. Histology of a choroidal melanoma with spindle melanoma cells; C: Epithelioid UM cells (8).

* Illustration from @ MAYO FOUNDATION FOR MEDICAL EDUCATION AND RESEARCH.

<https://www.mayoclinic.org/diseases-conditions/eye-melanoma/symptoms-causes/syc-20372371>

(Date of access: 02.04.2018)

2. Clinical presentation and risk factors

Clinical symptoms are often inconspicuous. Patients may present with visual acuity decrease, localised scotoma, photopsia, metamorphopsia, and color vision deficiency, depending on the properties of the tumors. These clinical complaints may be absent when the tumor derives from the peripheral area of the fundus. Increased intraocular pressure may occur in advanced stages due to the tumor volume augmentation, accompanied by red and/or puffy eye, ophthalmodynia, headache, and exophthalmos. Besides, an externally visible abnormality of the iris melanoma might be the main reasons for a patient's visit. Ophthalmoscopic findings, such as different levels of the elevated, oval and brown-coloured lesions, are indicative of a posterior choroidal melanoma. Once the apical part of grown tumor breaks through Bruch's membrane, a typical feature shaped as 'collar stud' or 'mushroom' is acquired. Associated signs such as subretinal fluid and exudative retinal detachment suggest the presence of an active tumor. Surface drusen (the yellow/white accumulations of extracellular deposits that locate between the RPE and inner Bruch's membrane of the eye) and RPE hypertrophy are characteristics of tumor chronicity (8).

The presence of choroidal nevus is highly correlated to the development of choroidal melanoma, which can be observed in up to 5% of the Caucasian

population (13). Distinct from cutaneous melanoma, exposure to ultraviolet radiation has not been clearly proven as a definitive environmental cause of UM. Other risk factors mentioned below imply a greater risk of distant metastasis of UM: larger tumors having more than 8 mm of apical dimension; tumors with epithelioid cells; BAP1 mutations that present in nearly 50% of UMs (9); chromosome 3 loss, which confers the worst prognosis, and the presence of chromosome 8 and 16 abnormalities. In contrast, chromosome 6p gain is significantly associated with a better outcome (46,103).

3. Existing approaches of UM treatment and corresponding limits

Currently, the major challenge in the management of UM is to improve its poor survival rate. Therapeutic modalities are performed based on the symptoms of patients, the tumor size, lesion location, degree of stromal penetration, presence of adjacent or systemic metastasis, metastatic extent, the fellow eye status, age and general health status of the patient, as well as the patient preference. Although the conventional treatments of primary tumor, such as extrascleral plaque brachytherapy, transpupillary thermal therapy (TTT), charged-particle therapy, local tumor resection, enucleation, and systematic adjuvant therapy with receptor inhibition or immune-modulating reagents, can stop local recrudescence in over 95% of the patients (7), they haven't been proven to effectively control further metastasis. Up to 50% of the patients develop metastasis predominantly in the liver within 10 years, and approximately with 89% metastasis to the liver (21,44). What follow in

the sections below are the general principles for the local therapy in the absence of metastasis and the guidelines which are recommended to the UM patients with evidence of distant metastasis.

3.1 Local treatments

Conventional managements, such as radiotherapy (brachytherapy and teletherapy) and transpupillary thermotherapy (TTT), can allow for the conservation of visual acuity in the patients with localized lesions. Other feasible management choices include local resection, enucleation or orbital exenteration.

3.1.1 Transpupillary thermotherapy (TTT)

TTT is a non-invasive treatment that induces tumor cell death by hyperthermia from an infrared laser beam, which is delivered through the pupil to the target tissue on choroid. Small tumors with a thickness of less than 4 mm and keeping a certain distance to the optic nerve or macula are conditions treatable with TTT. Additionally, it is also performed with extrascleral plaque brachytherapy as a combination modality therapy for small tumors (45), especially in the cases with tumor relapse. Though laser presents as a safer management compared to invasive surgery, it is limited to flat tumor (2.5 mm) and has a high local recurrence rates, which were reported to be 9% in the first year and 27% in the five-year follow-up (90).

3.1.2 Radiotherapy

Radiotherapy can be classified into two main forms: plaque brachytherapy and proton beam radiotherapy (or teletherapy). Brachytherapy refer to the application of a sutured Iodine-125 or Ruthenium-106 plaque to the sclera for several days, which is more commonly recommended as a vision salvaging approach for medium size UM (thickness of 2-8 mm and basal diameter of 8-16 mm) with a desired dose of radiation (70-100 Gy) (26). The Collaborative Ocular Melanoma Study (COMS), a prospective randomized trial, found no difference in the mortality rate of UM patients with tumors of 2.5-10 mm in apical height treated with plaque brachytherapy or enucleation (19). Five-year postoperative evaluations showed up to 46% recurrence rate and more than 18% mortality rates, with related complications include cataract, radiation retinopathy, maculopathy, neovascular glaucoma and exudative tumor response (5,49,65,89,95). Teletherapy or proton beam therapy refers to a projection of a beam of accelerated protons to irradiate and destroy the cancerous cells. The advantage of the teletherapy is that it is not limited by the certain size or location of the tumorous lesion as the brachytherapy (26). However, the following complications after irradiation and the secondary surgical treatment may not inevitable (31). Besides, clinical studies found no difference in metastasis-free or overall survival in the compared particle teletherapy to plaque brachytherapy (15,68).

3.1.3 Surgical resection

The surgical resection includes local resection, enucleation and exenteration. A large neoplasm, extensively recurrent tumors, optic disc invasion, loss of vision, and painful eye due to melanoma-induced glaucoma involvement, are crucial condition to perform enucleation. It is a surgical procedure involving the removal of the eyeball, insert of the orbital implant, with eye muscles and orbital contents still intact. The exenteration is recommended with the clinical evidence of the extrascleral extension (31). The difference between enucleation and exenteration is the former remove the entire eye ball with the remaining of the orbital contents, whereas the latter excise the all contents of eye socket involving ocular muscles, lacrimal gland system, optic nerve and orbital bones with the evidence of the extraocular invasion of the tumor. However, these have not been demonstrated to be of benefit for the prevention of the metastatic spread of UM (105). Five-year survival rates after enucleation were indicated as 84%, 68% and 47% for the small, medium-sized and large neoplasm, respectively (20). Certain study including 111 consecutive patients reported that primary enucleation led to more than 2 times higher of the 5- and 10-year mortality rates than the brachytherapy (49).

3.2 Treatment of metastatic disease

Circulating UM cells have been detected in patients who were clinically free of metastasis at diagnosis (97), suggesting that subclinical micrometastases may present at the time of diagnosis in these patients (50). The typical symptoms, such

as blurred vision, metamorphopsia, localized scotoma, photopsia, and partial visual field loss, do not present in every case. Approximately 30% of the patients are asymptomatic at diagnosis (104), which delays the early detection and timely managements. Due to the lack of efficient therapies, 5-year survival rates (81.6%) have not changed in the past three decades (92). Once metastasis occurs, it results in an approximate survival time of 12-14 months following diagnosis (105).

Liver is the most common target organ of UM metastasis, affecting around 89% of the patients (105). There is currently no standard remedial pattern for metastatic UM. Conventional regimens include liver-target therapy, systemic chemotherapy, immunotherapy and targeted therapy. Most of the remedial agents utilized for chemotherapy and immunotherapy are adapted for the treatments of cutaneous melanoma, such as the chemotherapeutics treosulfan and dacarbazine, cytotoxic T-lymphocyte-associated antigen 4 (CTLA-4) inhibitor ipilimumab, and anti-programmed cell death-1 (PD-1) receptor antibody Nivolumab. However, expected outcomes remain disappointing, with the response rate of 0-15% and the absence of an improvement in the survival rate (4,109).

Unfortunately, previous results of pathway-targeted therapies showed no better results than the treatments mentioned above, with less than 10% of the overall clinical response rate and 3.29 weeks of the median progression-free survival (7,15,19,65). UM is activated by mutated GNAQ/ GNA11 genes, which induce the constitutive activation of MAPK (mitogen-activated protein kinase) and PI3K/AKT signaling pathways. Several novel molecular therapies are targeting the

downstream effectors of these signaling pathways, such as the mitogen-activated protein kinase kinase (MAPKK or MEK) inhibitor selumetinib and trametinib, protein kinase C (PKC) inhibitor AEB071 (MAPK signaling pathway), AKT inhibitor GSK795 (PI3K/AKT signaling pathways), hepatocyte growth factor receptor tyrosine kinase c-Kit/c-Met inhibitor sunitinib and cabozantinib, and heat shock protein 90 (HSP90) inhibitor Ganetespib, which are recently under clinical investigation. These adjuvant therapies are still administered as ongoing clinical trials and none of them has been verified of metastasis free survival or overall survival benefits to date.

4. Pathogenesis

4.1 Rho/ Rho-kinase/ YAP signaling pathway underlying the GNA-driven UM development

The molecular profile of UM is composed of various chromosomal abnormalities and somatic gene alterations. Up to 83% of primary UMs are triggered by mutations in the GNAQ (Guanine nucleotide-binding protein subunit alpha-Q) or GNA11 (Guanine nucleotide-binding protein subunit alpha-11) genes encoding the heterotrimeric G protein alpha-subunits Gαq and Gα11, respectively, which lead to the conversion of these signaling proteins into a constitutively active form (99). In a study of oncogenic mutations in 123 primary UM patients, 47% harbored mutations in the GNAQ gene and 44% had mutations in the GNA11 gene (17). These two mutations are also predicted to be genetically initiating events in the tumorigenesis

of UM (36,75). However, the precise molecular mechanisms underlying the GNA-driven UM development still remain to be elucidated. Recently, the mutations in Gαq/11 were found to be correlated with an increased activity of the YAP protein through the Rho/Hippo signaling pathway, which promoted UM cell growth (24,112). YAP acts as a transcriptional coactivator in most proliferating cells. The YAP-dependent transcription is initiated through the activation of a Gαq-regulated guanine nucleotide exchange factor, Trio and the subsequent activation of the small GTPases RhoA and Rac1, promoting the polymerization of globular (G) actin to filamentous (F) actin. F-actin can bind angiomin (AMOT), leading to the nuclear translocation of YAP and activation of YAP-dependent gene transcription, which promotes excessive proliferation (24). (Figure 2)

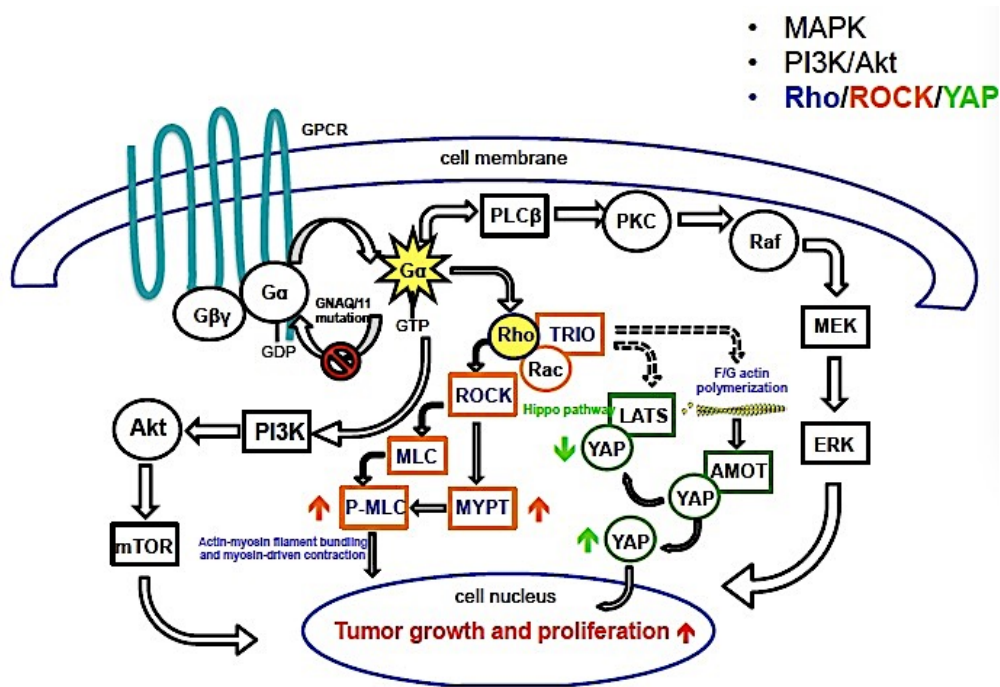


Figure 2. Proposed mechanism leading to the development of UM: G α activated signaling pathway and the Rho/Rho-kinase/YAP pathway. In UM cells, the mutations in oncogenic GNAQ/11 were found to be correlated with an increased activity of the G protein alpha-subunits (G α). The YAP activation occurs through active G α protein signaling to Trio, which promotes the polymerization of globular (G) actin into filamentous (F) actin via Rho/Rac. F-actins can bind angiomin (AMOT) and further release YAP to enter the nucleus. The Rho/Rho-kinase signaling pathway is an important regulator of actin cytoskeleton organization, and implicated in numerous aspects underlying cancer progression, including proliferation, migration, adhesion, matrix remodelling, angiogenesis, and gene expression. Rho-kinase might therefore become a noteworthy pharmacological target for the inhibition of UM metastasis (24).

4.2 Synthetic Rho-kinase inhibitors to suppress the pathological Rho-kinase activity in UM

As an important regulator of actin cytoskeleton organization, Rho/Rho-kinase pathway is implicated in numerous aspects underlying cancer progression, including proliferation, migration, adhesion, matrix remodeling, angiogenesis, and gene expression (102). Accordingly, the pharmacological inhibition of Rho-kinase with the moderately selective synthetic inhibitor Y-27632 resulted in a decreased motility and survival of cultured UM cells (85). Our preliminary data also demonstrated that the treatment with H-1152, the most specific of the currently available synthetic Rho-kinase inhibitors, suppressed the proliferation of UM cells in response to the conditioned medium of human hepatocytes (98). Rho-kinase therefore emerges as a noteworthy pharmacological target to interfere with multiple cellular events underlying UM metastasis. (*Figure 3*) Rho-kinase inhibitors, such as fasudil and Y-27632, are non-selective inhibitors, which non-specifically suppress

both ROCK1 and ROCK2 by targeting their ATP-dependent kinase domains and competing with ATP for binding to their catalytic sites (32,58). (Table 1) However, there is no work specifically focusing on the availability of naturally occurring Rho-kinase inhibitors so far.

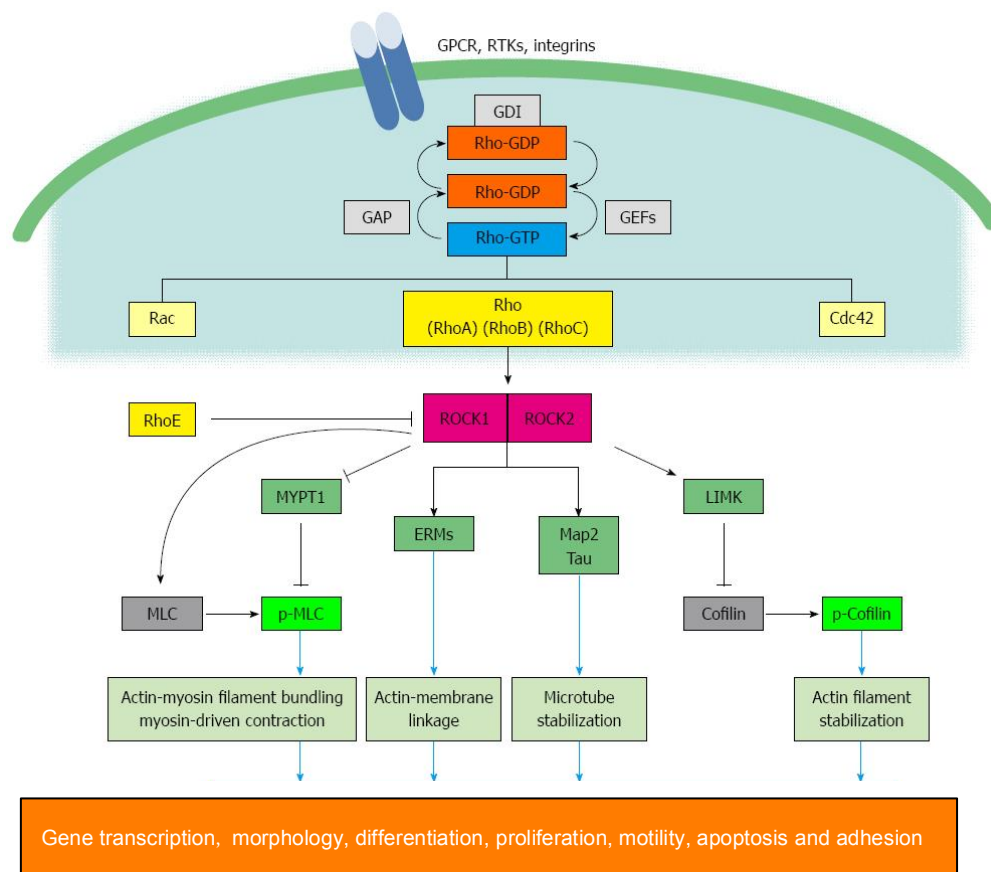


Figure 3. Rho/ Rho-associated coiled-coil containing protein kinase (Rho-kinase/ROCK) signaling pathway and their downstream cellular functions. The activation of Rho-GTPase proteins are regulated by guanine-nucleotide-exchange factors (GEFs) and GTPase-activating proteins (GAPs). Activated Rho-GTPase acts on Rho-kinase/ROCK, which phosphorylates various downstream proteins. The Rho-kinase-dependent phosphorylation of myosin light-chain (MLC) promotes actomyosin contraction. Activated LIMK by Rho-kinase induces the phosphorylation and inactivation of the cofilin, suppressing the disassembly of actin filaments. These two events play a vital role in cytoskeleton remodeling, cell adhesion motility and adhesion. Collectively,

Rho/Rho-kinase and their downstream effectors carry out many important cellular activities, that render them as potential therapeutic targets to inhibit tumorigenesis and metastasis (66).

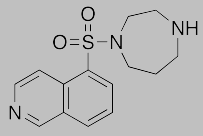
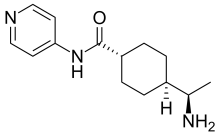
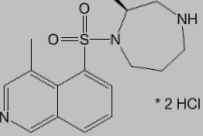
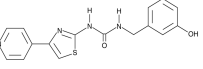
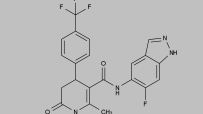
Name	Chemical Structure	Target	Cancer cells/ Cell lines tested
Fasudil (HA1077)		ROCK1/2 PKA PKG PKC	Leukemia, UM-UC3, T98G, U87MG, U251, A549, 95D, A2780, B16
Pyridines (Y-27632)		ROCK1++ ROCK2+	Leukemia, MDA-MB-231, SUM 1315, MCF-7 ,MDA-MB-231,HCT116, HT29, LN-18, Li-7, A549, A2780, SKOV3, PC3, LNCaP, CB0140C12, B16F1
H-1152 (di-methylated variant of fasudil)		ROCK1/2 PKA, PKG, PKC	B16F10
RKI-1447		ROCK1+++ ROCK2+++	H-1299, MDA-MB-231 MDA-MB-468
GSK429286A		ROCK1+++ ROCK2++	NRAS-mutant

Table 1. Several Rho-kinase inhibitors in various cancer model studies (14)

* "+" indicates inhibitory effect. Increased inhibition is marked by a higher "+" designation. Images of the chemical structures of inhibitors were obtained from: <http://www.selleckchem.com/ROCK.html>

5. Phytochemical therapy

Since the effects of canonical interventions are limited for the UM in metastatic phases, prevention before metastasis seems to be the priority needed to be solved. Currently natural compounds play an important role in numerous biomedical applications, especially in anticancer therapies. More than 60% of the clinically applied anticancer agents are derived from natural sources as potential therapeutics with lower side effects (16).

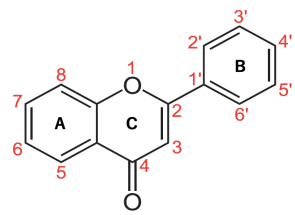
Safety is indeed the major concern for synthetic chemotherapeutic drugs. An ideal compound for both chemoprevention and therapy should be nontoxic, easily extractable, economical, highly efficient, and with a low drug resistance (2). Natural phytochemicals were found to be safe in long-term human diet consumption and many of them could exhibit potential chemopreventive and anti-tumor effects in preclinical studies (3,33). Moreover, most natural compounds hit multiple targets compared to synthetic chemotherapeutics (3,33). Therefore natural phytochemicals might aid in the development of effective and rational strategies with lower side effects for cancer remedy.

5.1 Flavonoids and their promising bioactive properties

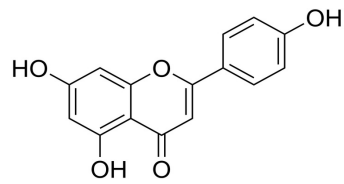
Flavonoids are the most common and widely distributed polyphenolic compounds, which are ubiquitously present in foods of plant origin. The flavonoid group is comprised of approximately 5,000 compounds (96) that are defined chemically as substances composed of two benzene rings (A, B) and a heterocyclic ring (C) (structurally abbreviated as C6-C3-C6). Accordingly, flavonoids are generally

classified into six subclasses: flavones, flavanols (catechins), flavanones, isoflavones, flavonols, and anthocyanins, depending on the degree of oxidation of the C in position 4, the hydroxylation pattern, and the substitution of the C3 position (96). *(Figure 4A)*

Flavonoids display various biological activities, including anti-allergic, anti-viral, anti-inflammatory, anti-oxidant, anti-tumor, and vasodilatory effects (38,56,60,61). Epidemiological studies also indicated that the dietary intake of total flavonoids is usually inversely correlated with the cancer risk (72). Interestingly, flavonoids seem to share a certain structural similarity to adenosine and the synthetic Rho-kinase inhibitors Fasudil and H-1152. *(Figure 4, Table 1)* Based on this similarity, flavonoids might occupy the ATP-binding domains of Rho-kinase and exert certain analogous biological effects as the Rho-kinase inhibitors mentioned above, which deserves further investigation.



A



B



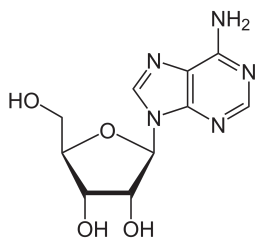
Parsley



Chamomile



Red wine



C

Figure 4. (A) Molecular structure of flavonoids. (B) Chemical structure of the flavonoid apigenin, which is highly abundant in parsley, chamomile and red wine. (C) Molecular structure of adenosine

5.2 Tanshinone IIA

Tanshinone IIA (*Figure 5*) is a lipid-soluble phenanthrene-quinone compound isolated exclusively from *Salvia miltiorrhiza* Bunge (Danshen in Chinese) and highly valued in traditional Chinese medicine for more than 2000 years (106), especially in the clinical application in cardiovascular and cerebrovascular disorders (12). Tanshinone IIA could promote anti-inflammatory (47), anti-oxidative (82), neuroprotective (53), antiangiogenic (55), and antifibrotic (107) activities. The anticancer potentials of Tanshinone IIA, however, have only been recognized in recent years. *In vitro* studies found that Tanshinone IIA could suppress the proliferation, migration, and viability of various tumor cells, inducing cell cycle arrest and apoptosis (12,27,70). Tanshinone IIA could also down-regulate the myosin phosphatase and vascular endothelial growth factor (VEGF) partly by the Rho/Rho-kinase pathway (57) and suppress actin cytoskeleton rearrangement and stress resistance during the tumorigenesis of human hepatocellular carcinoma cells (62). However, there is so far no study focusing on the inhibitory potential of tanshinone IIA on UM cells.

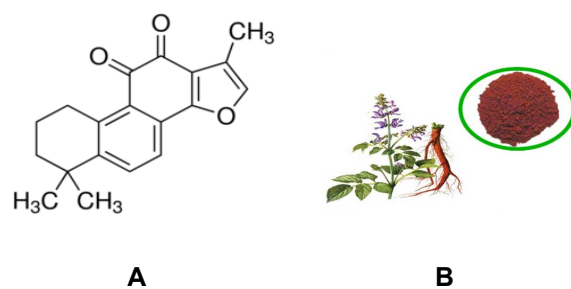


Figure 5. Chemical structure of TAN IIA (A), a lipid-soluble phenanthrene-quinone compound isolated exclusively from *Salvia miltiorrhiza* Bunge (Danshen in Chinese) (B).

5.3 Apigenin

Apigenin (4', 5, 7-trihydroxyflavone) is a natural phytochemical compound and the major flavone that can be found in many vegetables, especially parsley, celery, chamomile, and red wine (83). (Figure 4B) Apigenin could exert significant anti-proliferative, anti-oxidant, anti-inflammatory, and anti-neoplastic effects (87). Apigenin could also induce apoptosis and suppress the metastatic activities of various tumor cells by interfering with cellular events that are mainly regulated by the Rho-kinase (71,78,91,101). Yet, similar to tanshinone IIA, there is so no study on the therapeutic potential of apigenin for UM treatment.

6. Research purpose

The biggest challenge in the management of UM is to prevent the metastasis and thus improve the survival rate of patients. Rho/Rho-kinase/YAP signaling pathway is recently proven to be involved in the growth of UM cells by controlling several cellular events, such as proliferation, motility, and apoptosis. However, there are currently no synthetic Rho-kinase inhibitors which are clinically approved for the treatment of UM patients.

Flavonoids are natural phytochemical metabolites, which are widely abundant in plants and which could exert suppressive effects on numerous cancer cell types. However, no studies have elucidated yet, whether certain flavonoids can prevent UM cell growth and to what extent the modulation of the activities of Rho-kinase and YAP would be involved in this process.

In our study, we investigated for the first time the *in vitro* efficacy of tanshinone IIA and apigenin as potential inhibitors of the growth and metastatic activities of the UM cell line 92.1, which harbors the Q209L mutation in the GNAQ gene. We also evaluated the outcomes of flavonoid treatment on the extent of Rho-kinase dependent events in UM cells to elucidate the possible underlying mechanisms. We are therefore trying to develop a natural, efficient, affordable, and immediately available pharmaceutical therapy with lower side effects for UM patients. [\(Figure 6\)](#)

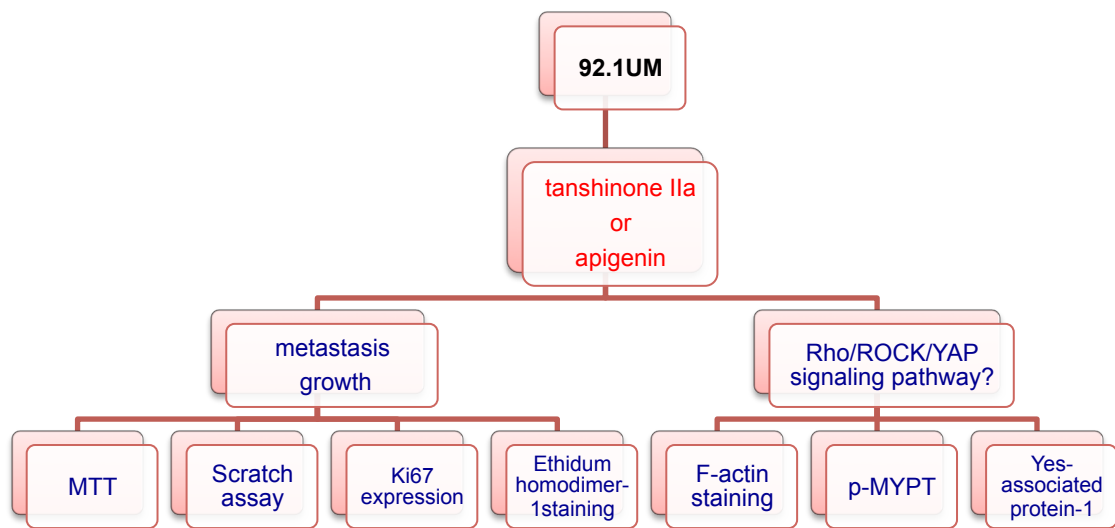


Figure 6. Study design: 92.1 cells were treated with tanshinone IIA or apigenin at a concentration range of 1.5-100 μ M. Viability and optimal concentration of test substances were evaluated by the MTT assay. Cell damage was determined by ethidium homodimer-1 staining. Organization of the actin cytoskeleton was analyzed by phalloidin staining. Migration was assessed by the scratch assay. Proliferation was determined by Ki67 immunostaining. Activity of Rho-kinase was analyzed by the immunostaining of myosin phosphatase target subunit 1 (MYPT1), the main downstream target of Rho-kinase, and phosphorylated Thr-696 (p-MYPT), one of the major Rho-kinase dependent phosphorylation sites on MYPT1. We also estimated the activation of YAP-1 (yes-associated protein-1) in response to these two flavonoids.

METHODS

Cell culture

UM cell line 92.1, which harbors the UM specific hotspot mutation Q209L in the GNAQ gene (30), was generated from the primary tumor of a female patient (18). The cells between the 9th and 19th passages were used for the experiments. Cells were grown in normal culture medium (RPMI-1640 with 2mM L-Glutamine, 10% serum, 100 Units/ml penicillin, 100 µg/ml streptomycin) in 75 cm² culture flasks at 37°C with 5% CO₂ and subcultured after reaching up to 70% confluence. Culture medium was replaced by two-third every 2-3 days.

MTT assay

The MTT test is a colorimetric assay for estimating cell metabolic activity by measuring the conversion of the tetrazolium dye MTT 3-(4,5-dimethylthiazol-2-yl)-2,5-diphenyltetrazolium bromide to insoluble formazan, which has a purple or dark blue color, under the action of NAD(P)H-dependent cellular oxidoreductase enzymes in the viable cells (6).

UM 92.1 cells were seeded into 96-well cell culture plates at a density of 8000 cells/well and incubated without (0) or with tanshinone IIA or apigenin at the indicated concentrations (1.56, 3.12, 6.25, 12.5, 25, 50, 100 µM) in normal culture medium (containing 10% serum) for 3 days. A group of cells were incubated in medium containing 0.5% serum as a negative control for cell growth. The vehicle group was incubated with normal culture medium containing dimethyl sulfoxide

(DMSO), which is the solvent used for dissolving tanshinone IIA or apigenin), at 1:500 dilution, corresponding to the concentration of DMSO in the 100 μM tanshinone IIA or apigenin groups. After 3 days, MTT solution (5 mg/ml) was added into cells and incubated for 3.5 hours. Cell solutions were discarded and replaced with 100 μL /well lysis solution (100% DMSO). The plate was shaken vigorously for 15 minutes and the absorbance values at 544 nm were measured with a spectrophotometric microplate reader. The background values of the negative control (row B) were subtracted from the absorbance values of all the test groups.

(Figure 7)

	2	3	4	5	6	7	8	9	10	11	
B	0.5%UMM	10%UMM	1.56	3.13	6.25	12.5	25	50	100	DMSO	
C	0.5%UMM	10%UMM	1.56	3.13	6.25	12.5	25	50	100	DMSO	
D	0.5%UMM	10%UMM	1.56	3.13	6.25	12.5	25	50	100	DMSO	
E	0.5%UMM	10%UMM	1.56	3.13	6.25	12.5	25	50	100	DMSO	
F	0.5%UMM	10%UMM	1.56	3.13	6.25	12.5	25	50	100	DMSO	
G	0.5%UMM	10%UMM	1.56	3.13	6.25	12.5	25	50	100	DMSO	

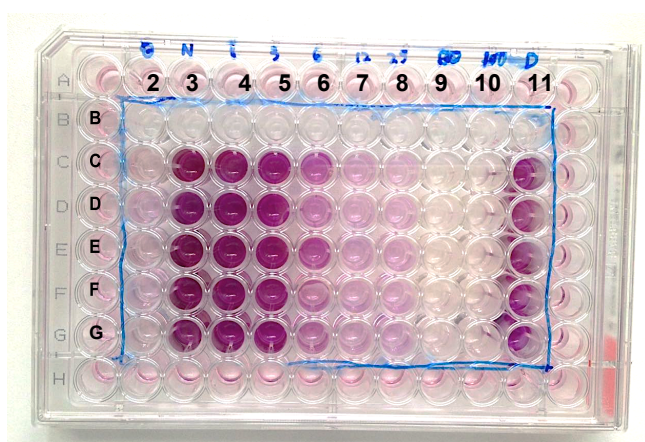


Figure 7. Template illustrates the different concentrations of test substances(μm) in 96-well plate.

Groups with 0.5% FBS (rank 2) and 10% FBS (rank 3) inside medium served as the negative and positive controls, respectively. DMSO (rank 11) at the same concentration used for dissolving 100 μM of the flavonoids served as the vehicle control. The wells on row B treated without MTT solution served as the background controls.

Survival test (Ethidium homodimer-1 staining)

Ethidium homodimer-1 (EthD-1) is a high-affinity fluorescent nucleic acid stain (Excitation: ~ 528 nm, Emission: ~ 617 nm) which cannot penetrate intact cell membranes and presents a weak fluorescence. Once the integrity of cell membrane has been damaged, as in the case of dead or damaged cells, EthD-1 penetrates the cell membrane, binds to DNA with high affinity and labels the cell with highly enhanced 40-fold red fluorescence. This dye is excluded from cells with an intact membrane and thus was used as an indicator of the extent of cell damage in our study.

92.1 cells were seeded into fibronectin coated (coating density: $4 \mu\text{g}/\text{cm}^2$) 12-well chamber slides at the seeding density of 1.5×10^4 cells/well (250 μl cell suspension per well). After overnight incubation, cells were treated with tanshinone IIA or apigenin with the same treatment methods as previously described below. (*Figure 8*) 0.5% FBS medium served as a control group for reduced cell growth. An additional group was treated with phosphate-buffered saline (PBS) after overnight incubation instead of test substances or medium as a positive control, where cells were deprived of essential nutrients (represented as the first well labeled green in *Figure 8*). Cells were rinsed with PBS after 3 days incubation and then incubated

with 100 μ l/well of 2 μ M Ethidium homodimer-1 (diluted in PBS at the ratio of 1:1000, protected from light) for 15 minutes under room temperature. Cells were fixed with 2% and 4% paraformaldehyde(PFA)-PBS solutions for 10 minutes each successively. After three times washing with PBS, the blocking buffer was applied for 30 minutes. Cells were incubated with the DAPI-PBS solution (0.5 μ g/ml, 100 μ l/well) for 10 minutes, for nuclear staining. After discarding the DAPI solution, the chambers were removed. The slides were then rinsed in a cuvette with PBS for 5 minutes, and covered with Mowiol-coated 60-mm coverslips. The cells were visualised by fluorescence microscopy using the appropriate filters (DAPI: excitation BP360/40, suppression BP470/40; EthD-1:excitation BP620/60, suppression BP700/75). Quantification of the value of intensities of ethidium homodimer-1 stainings was performed using the Fiji software on the fluorescent images.

No UMM change	0.5%FBS UMM	10%FBS UMM	1.56	3.12	6.25
12.5	25	50	100	DMSO	PBS

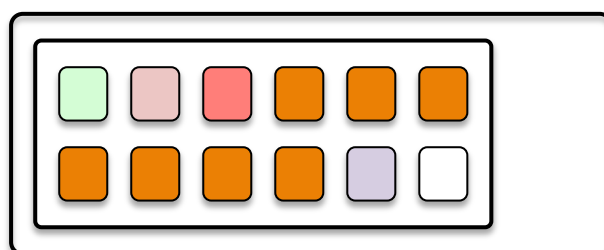


Figure 8. Template illustrates the different concentrations of tanshinone IIA or apigenin (μ m) in a 12-well chamber slide (orange). Cells that were incubated with medium containing 0.5% FBS (light pink) or 10% FBS (dark pink) served as controls. DMSO (purple) of the same concentration as

those used for dissolving the test substances served as vehicle control. (Green: no medium change. White: PBS. UMM=uveal melanoma medium)

Phalloidin staining (F-actin/microfilament staining)

12-well chamber slides were coated with fibronectin and seeded with the 92.1 cells as mentioned above. After overnight incubation, cells were treated with tanshinone IIA or apigenin with the same treatment methods as described above. (*Figure 8*) 0.5% FBS medium served as a control group for reduced cell growth. One group was treated with PBS solution after overnight incubation instead of test substances or medium as an additional control for cell starvation/damage. Cells were rinsed with PBS after three days incubation and fixed with 2% and 4% PFA-PBS solutions for 10 minutes each. The blocking buffer was applied for 30 minutes after PBS washing. Cells were incubated with Alexa Fluor 488-conjugated phalloidin for 1 hour under room temperature, except for one group (arranged as the first well of the chamber slide, illustrated as green in *Figure 8*), which was treated with only the blocking buffer as the negative control. After 3 times rinsing with PBS, cells were incubated with the DAPI solution (0.5 µg/ml, 100 µl/well) for 10 minutes, for nuclear staining. After discarding the DAPI solution, the chambers were removed. The slides were then rinsed in a cuvette with PBS for 5 minutes, and covered with Mowiol-coated 60-mm coverslips. The cells were visualised and photographed by fluorescence microscopy using the appropriate filters (DAPI: excitation BP360/40, suppression BP470/40; Phalloidin: excitation BP460/40, suppression BP527/30). Images at the magnification of 400x were quantified by measuring the values of the

areas of complete microfilament staining of all the cells in the view field using the Fiji program. The results of three independent experiments were collected and presented as the mean±standard error of the mean (SEM).

Scratch-wound healing assay

92.1 cells were seeded in 24-well plates at a concentration of 5×10^4 cells/well. The medium was changed every 2-3 days until the confluence reached 80-90%. Cells were washed with PBS twice and a wound line was scratched in the middle of the cell monolayer using a new, sterile 1000 µl pipette tip in each well. Cells were washed with 1× Hanks' Balanced Salt Solution twice before being treated with tanshinone IIA or apigenin at the concentrations as described below. (Figure 9) Microphotographs of the marked regions along the wound area were obtained at 0 and 48 hours after scratching using a phase-contrast microscope at a magnification of 50x. The initial wound area and the area unoccupied by cells were measured by using the Fiji program. The extent of cellular invasion was determined as the percentage ratio of the healed wound area and the initial wound area calculated following the formula below.

$$\text{the ratio of healed wound area (\%)} = \left(1 - \frac{\text{unhealed wound area}}{\text{initial wound area}}\right) \times 100\%$$

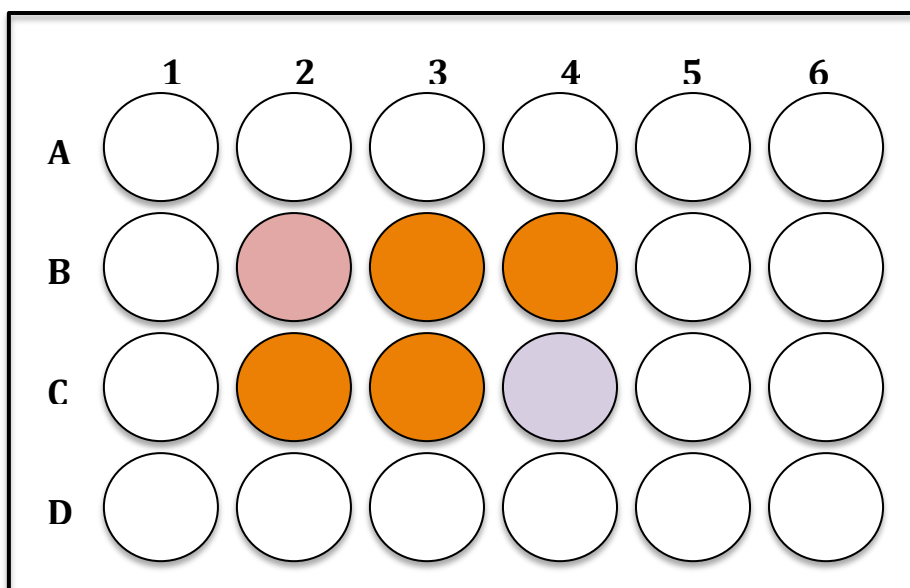


Figure 9. Template illustrates the different concentrations of test substances (μM) in a 24-well chamber plate. The concentrations of tanshinone IIA are 3.13, 6.25, 12.5 and 25 μM while apigenin was introduced at 12.5, 25, 50 and 100 μM (orange). Cells incubated in 10% FBS medium served as the positive control group (pink). DMSO (purple) of the same concentration as those used for dissolving the test substances served as vehicle control.

Immunostaining

92.1 cells were seeded in fibronectin coated 12-well chamber slides (coating density: $4 \mu\text{g}/\text{cm}^2$) at the seeding density of 1.5×10^4 cells/well (250 μl cell suspension per well) or uncoated 8-well polycyanoacrylate (PCA) slides at the seeding concentration of 4×10^4 cells/well. After overnight incubation, cells were rinsed with PBS twice and treated with tanshinone IIA or apigenin at the indicated concentrations. (Figure 8 and 10) 0.5% FBS medium served as negative control groups. Cells were rinsed with PBS after 1-3 days incubation and fixed with 2% and 4% PFA-PBS solution. The blocking buffer was applied for 30 minutes after three times washing with PBS. The primary antibodies were diluted with blocking buffer

in the ratios as indicated in [Table 2](#). Cells were incubated with the primary antibody overnight (16-18 hours) at 4°C or for one hour under room temperature, with the exception of the negative control, which was treated with just the blocking buffer. After 3 times rinsing with PBS, cells were incubated with Alexa Fluor 488 conjugated secondary goat anti-rabbit IgGs, diluted in the blocking buffer in the ratio of 1:200, for one hour under room temperature. After three times rinsing with PBS, cells were incubated with DAPI solution for nuclei staining. DAPI was aspirated out of the chamber slide. Chamber of the slide was removed before being immersed in PBS for 10 minutes. Slide was covered with 60-mm Mowiol-coated coverslips. The cells were visualised by fluorescence microscopy using the appropriate filters (DAPI: excitation BP360/40, suppression BP470/40; Phalloidin: excitation BP460/40, suppression BP527/30). Images at the magnification of 400x were acquired and positive cells were quantified using the Fiji program as described below.

Concentration of tanshinone IIA (μM) in YAP-1 immunostaining:

No UMM change	0.5%FBS UMM	10%FBS UMM	6.25
12.5	25	50	DMSO

A

Concentration of apigenin (μM) in YAP-1 immunostaining:

No UMM change	0.5%FBS UMM	10%FBS UMM	12.5
25	50	100	DMSO

B

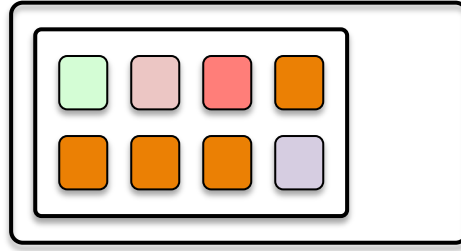


Figure 10. Templates illustrate the different concentrations of test tanshinone IIA (A) and apigenin (B) (μm) in 8-well chamber slide (orange). Cells treated with medium contained 0.5% FBS (light pink) or 10% FBS (dark pink) were served as the negative controls. DMSO (purple) of the same concentration as those used for dissolving test substances was served as vehicle control. (Green: no medium change. UMM=uveal melanoma medium)

Primary antibodies

Antigen	Type	Company	Catalog number	Dilution factor
Ki67	Rabbit IgG polyclonal	Abcam	ab15580	1:500
MYPT1+MYPT2	Rabbit IgG monoclonal	Abcam	ab32519	1:100
p-MYPT (phospho T696)	Rabbit IgG monoclonal	Abcam	ab59202	1:100
YAP1	Rabbit IgG monoclonal	Abcam	ab52771	1:150

Secondary antibody

Reactivity	Type	Label	Company	Catalog number	Dilution factor
Rabbit IgG	Goat IgG	Alexa 488	Abcam	ab150077	1/200

Table 2. The primary and secondary antibodies used in experiments.

Abbreviations: IgG, immunoglobulin G; MYPT, Myosin Phosphatase.

Range of Filter Cubes of the Leica Fluorescence Microscopy			
Filter cube	Excitation range	Excitation filter	Suppression filter
A4	UV	BP360/40	BP470/40
L5	Blue	BP460/40	BP527/30
Y5	Red	BP620/60	BP700/75

Table 3. The range of filter cubes of the Leica fluorescence microscopy used in experiments.

Quantifications of immunostainings

The cells were photographed by fluorescence microscopy with a minimum of 15 images/ well on 8-well chamber slide or 20 images/ well on 12-well chamber slide. Quantifications of the staining intensity were performed using the Fiji software on the images by marking all the cells, which were completely present in the field of view. To better identify the boundaries of cells that exhibit a very weak staining, the intensity of MYPT1+2 and p-MYPT were quantified on the merged images of the DAPI and tested protein stains, respectively, and the green intensity values were recorded from the histograms of marked regions. The green intensity of Ki67 and YAP-1 were obtained by marking the nuclear region on the merged images. The thresholds of the intensity of Ki67 staining were determined by the green intensity of the negative controls (incubated with the blocking buffer alone without the primary antibody). The percentage of the cells with positive Ki67 stain was defined as the intensity value higher than the threshold in all the cells with green staining.

The mean intensity of negative controls was subtracted from the intensity of test groups for all the immunostainings.

Evaluation of cell cycle arrest by measuring the integrated density of the DNA-binding dye DAPI

The analysis of different cell cycle phases were performed by measuring the DNA levels in the fluorescence microscopy images of the 92.1 cells treated with or without tanshinone IIA or apigenin for 3 days, which were all selected from three sets of experiments in our study. The cell cycle phases are defined as the Sub G1 stage (cells with DNA loss), G0/G1 (Quiescent / Gap 1) stage, S (DNA synthesis) stage, and G2/M (Gap 2 / Mitosis) stage. The integrated density of the DNA-binding dye DAPI staining in the nucleus region of each cell was measured using the Fiji software (n= minimum 50/20 nuclei/group). The nuclei located at the edges of the images were filtered out of quantifications. The thresholds for the classification of cell cycle phases were calculated by the frequency distributions of the DAPI integrated density of the nuclei in untreated cells using the Excel software. Afterwards, the percentages of cells belonging to each phase of the cell cycle were quantified in the untreated group. Accordingly, the DAPI integrated densities of the treated cells were sorted to the corresponding cell cycle phases based on the threshold settings of the untreated cells. The methods above are followed using the principle and protocol introduced by Roukos V, et al (84).

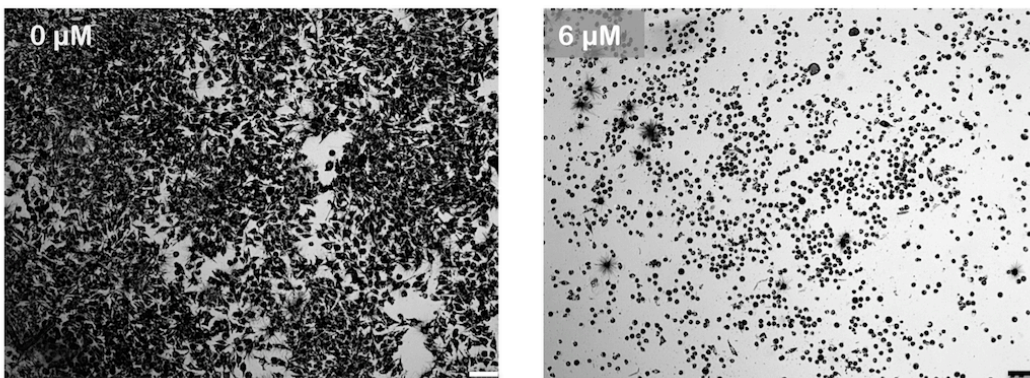
Statistical Evaluation

Statistical analysis was performed using the Microsoft Excel software. The two-sided Student's *t*-test was applied for comparing the test groups and negative controls, assuming equal variance among the samples. The *P* values less than 0.05 were considered as statistically significant.

RESULTS

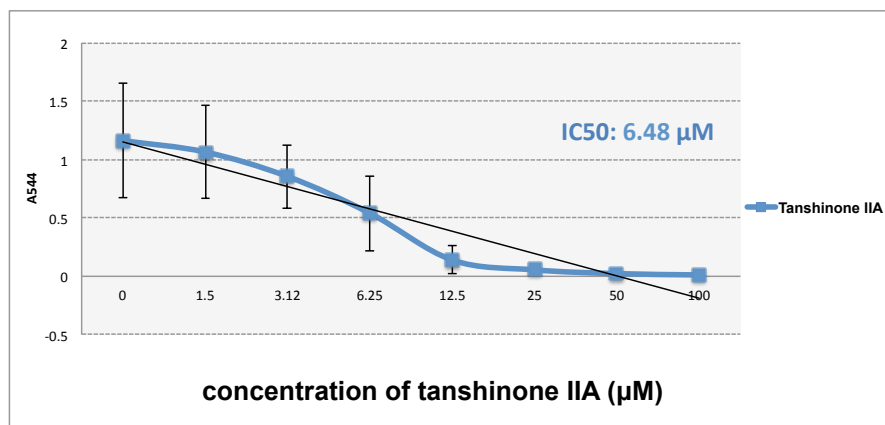
MTT assay: Optimal concentration of the flavonoids

Tanshinone IIA led to a significant and dose-dependent reduction of metabolically active 92.1 cells at the concentration of 12.5 μM onwards after 72 hours. Compared to tanshinone IIA, apigenin had a weaker impact on UM cells and a significant reduction in cell growth was observed at the higher tested concentrations (50-100 μM). (Figure 11)

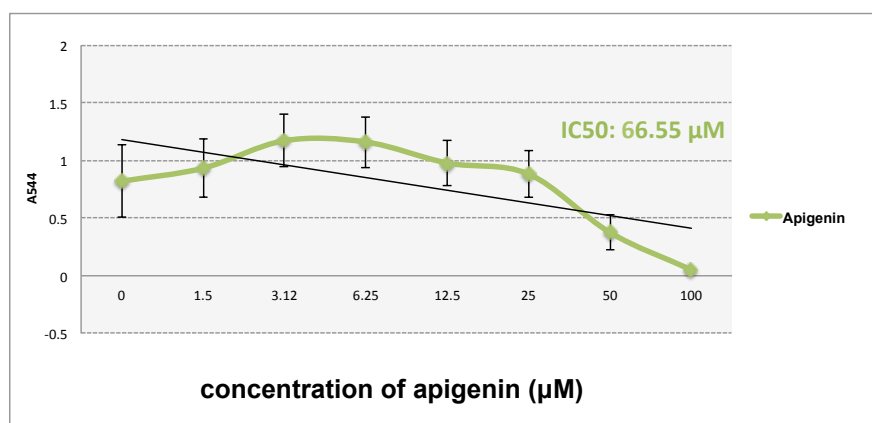


A

B



C



D

Figure 11. Tanshinone IIA led to a significant and dose-dependent reduction of metabolically active 92.1 cells after 72 hours. Phase-contrast images of the cells in normal culture medium (A) or in medium with 6 µM tanshinone IIA (B) after incubation with the MTT dye for 3 hours. Bar= 100 µm. (C) Histograms of tanshinone IIA represent the mean ± standard error of mean (SEM) of n=4 independent experiments. IC50 (Inhibiting concentration)=6.4821 µM. (D) Quantification of metabolically active cells after apigenin treatment. Data represent the mean ± SEM of n=5 independent experiments. IC50=66.54825 µM

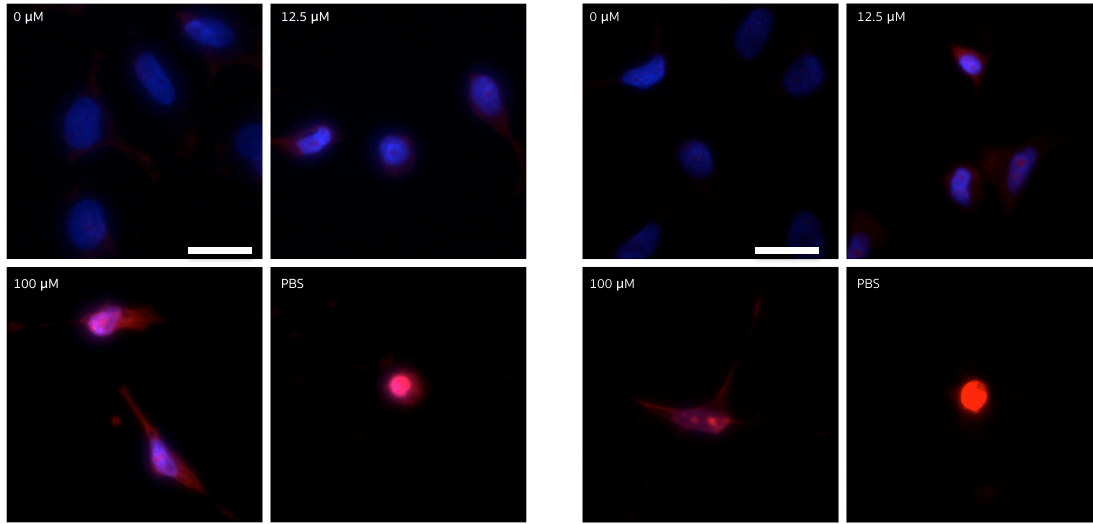
Survival test: ethidium homodimer-1 staining

Cell damage was evaluated by the extent of staining with the membrane-impermeable fluorescent dye ethidium-homodimer-1. A significant and dose-dependent increase in the uptake of this dye was observed in the test groups treated with tanshinone IIA (from 25 µM onwards) and apigenin (from 12.5 µM onwards). These results indicated that both test substances could induce a dose-dependent impairment of the plasma membrane integrity and viability of 92.1 UM cells. (Figure 12)

Tanshinone IIA

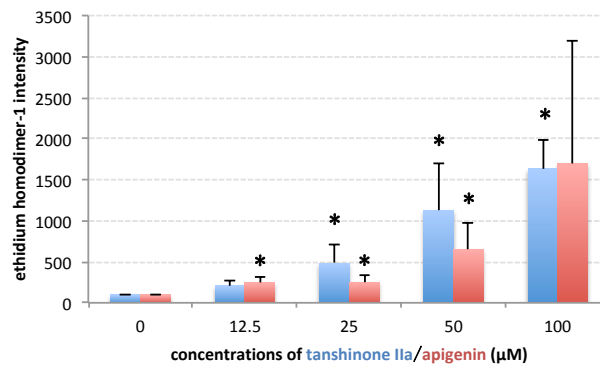
Apigenin

DAPI/ Ethidium homodimer-1



A

B



C

Figure 12. Increase in cell permeability and damage in response to Tanshinone IIA and apigenin. 92.1 cells were treated with tanshinone IIA or apigenin for 3 days and cell damage was assessed by ethidium homodimer-1 staining. Fluorescent images demonstrated that tanshinone IIA (A) and apigenin (B) led to a significant increase in the uptake of this dye in the experimental groups compared with the control group. Bar=25 μm. (C) Quantification of ethidium homodimer-1 intensity. Data represent the mean ± SEM of n=3 independent experiments of tanshinone IIA (blue) and apigenin (red), respectively. *P* values compared to control group. **P*<0.05.

Morphological changes in response to tanshinone IIA and apigenin estimated by the staining of actin microfilaments

The morphology of the 92.1 cells after the incubation with flavonoids was assessed by the staining of actin microfilaments. Tanshinone IIA and apigenin led to a dose-dependent decrease in the amount of actin microfilaments, which became significant at a concentration of 50 μM ($P=0.018$ and 0.049 respectively, compared to control) and 100 μM ($P=0.014$ and 0.044 respectively, compared to control). Cells incubated with such high concentrations of the flavonoids exhibited apoptotic morphology with shrinkage of cell size and loss of filamentous actin. Interestingly, cells treated with the intermediate concentrations of tanshinone IIA and apigenin exhibited long, branch-like dendritic protrusions, which are characteristic of the quiescent, differentiated melanocytes in healthy tissue, indicating that these flavonoids at intermediate concentrations might promote cellular differentiation to a certain degree. (*Figure 13*)

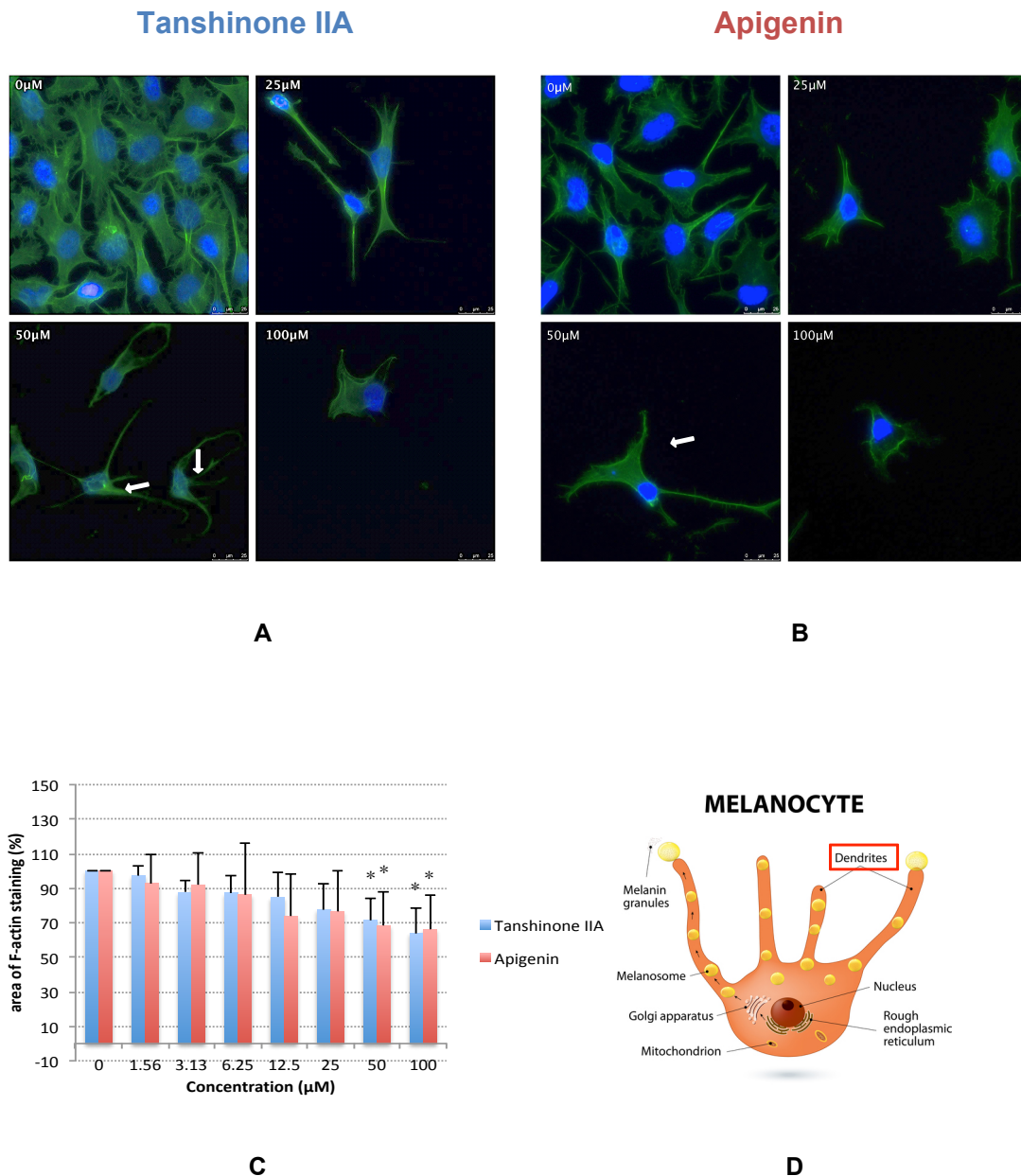
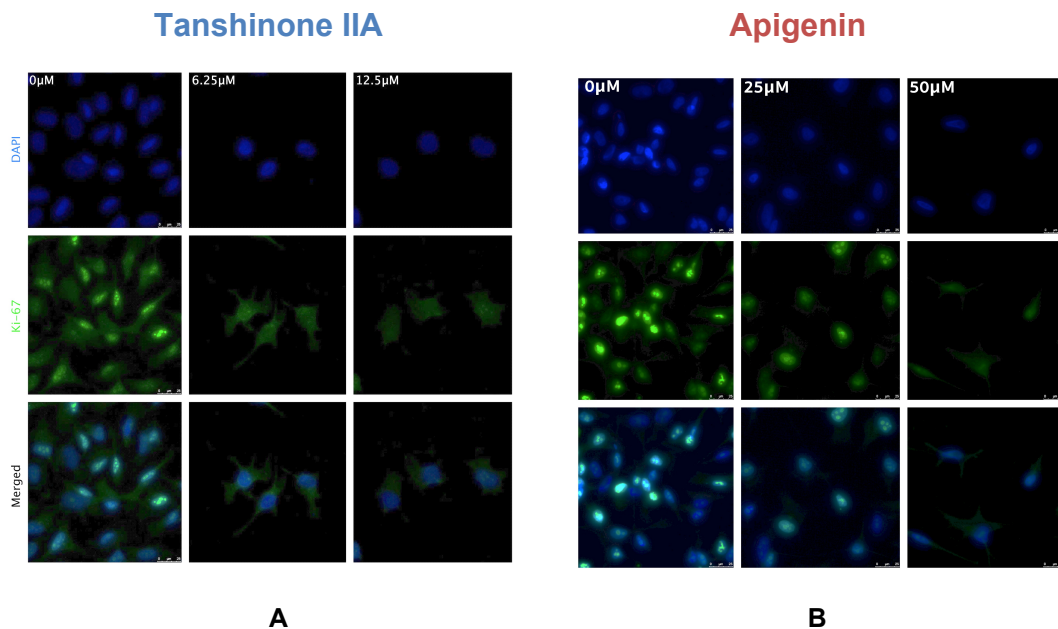


Figure 13. Staining of the actin filaments with fluorescently labeled phalloidin in the 92.1 cells treated with tanshinone IIA and apigenin for 72 hours. Fluorescence microscopy images demonstrate the disruption of actin microfilaments in response to tanshinone IIA (A) or apigenin at high concentrations (B), manifested as the shrinkage of cell size and the weakening of the staining intensity. (C) Quantification of the area value of phalloidin represent the mean \pm SEM of $n=3$ independent experiments of tanshinone IIA (blue) and apigenin (red), respectively. P values compared to control group. $*P<0.05$. Cells treated with the intermediate concentrations of flavonoids exhibited long, dendritic protrusions (Indicated by the arrows in A and B), similar to the normal, differentiated melanocytes (D). (Source of illustration D: <https://ghr.nlm.nih.gov/condition/giant-congenital-melanocytic-nevus>. Date of access: 09.04.2018)

Anti-proliferative effect of the flavonoids assessed by Ki-67 immunostaining

Proliferation of 92.1 UM cells in response to tanshinone IIA and apigenin for 72 hours was determined by the Ki-67 immunostaining. A dose-dependent decrease in Ki-67 levels was observed in response to apigenin compared to the control group, which became significant at a concentration of 50 μM onwards ($P=0.040$ and 0.047 respectively, compared to the control). Incubation of the cells with 12.5 or 25 μM of tanshinone IIA also led to a significant decrease in the percentage of Ki67-positive cells ($P=0.008$ and 0.019 respectively, compared to control). However this effect diminished in the cells treated with higher concentrations of tanshinone IIA without reaching significance ($P= 0.420$ for 50 μM and $P=0.265$ for 100 μM tanshinone IIA compared to control). (Figure 14)



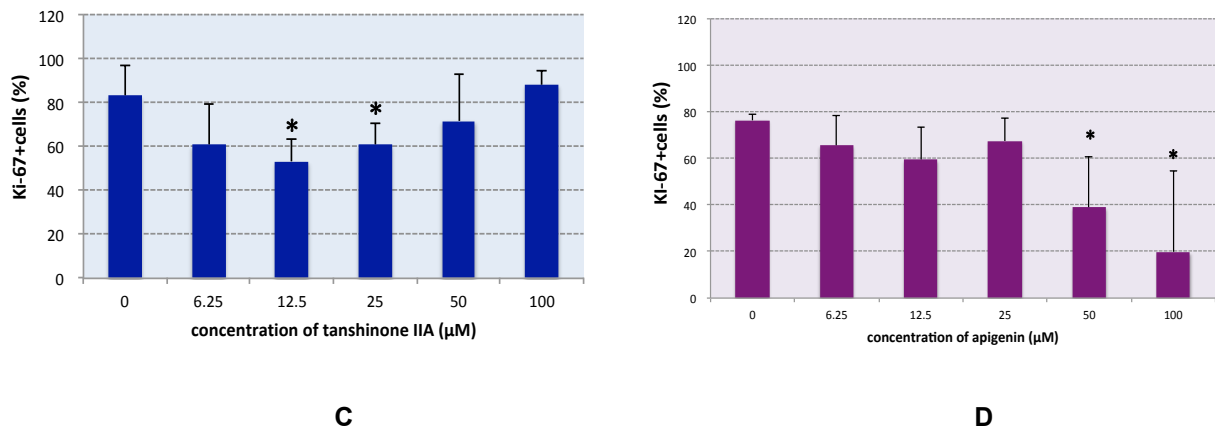


Figure 14. Ki-67 immunostaining of 92.1 cells treated with tanshinone IIA and apigenin for 72 hours. Images show a dose-dependent decreased expression of Ki-67 treated with tanshinone IIA (A) at the intermediate concentrations of 6.25 to 25 μM. Apigenin (B) had a weaker impact on the expression of Ki-67 in the UM cells, with a significant decrease occurring at a concentration of 50 μM onwards. Quantification of the percentage of Ki-67-positive cells in the groups treated with tanshinone IIA (C) or apigenin (D). Data represent mean ± SEM of three independent experiments. * $P < 0.05$ ** $P < 0.01$.

Cell Migration: Wound healing (Scratch) assay

Cell motility in response to the flavonoids was tested via the scratch / wound-healing assay, by creating a wound in the middle of a confluent cell layer and determining the extent of wound invasion with the cells after 48 hours. Untreated cells could efficiently repopulate the wound region, resulting in the coverage of 69.751-80.444% (TAN IIA) and 61.266-73.039% (apigenin) of the initial wound area after 48 hours. The invasion of the wound area was impaired in response to the flavonoids in a dose-dependent manner. Tanshinone IIA at 25 μM resulted in a significant decrease in wound coverage by 58.285% ($P = 0.029$ compared to control). Likewise, the treatment with 50 and 100 μM apigenin reduced the extent of cellular invasion by 36.138% and 24.045%, respectively,

compared to control ($P=0.003$ and 0.001 , respectively). (Figure 15)

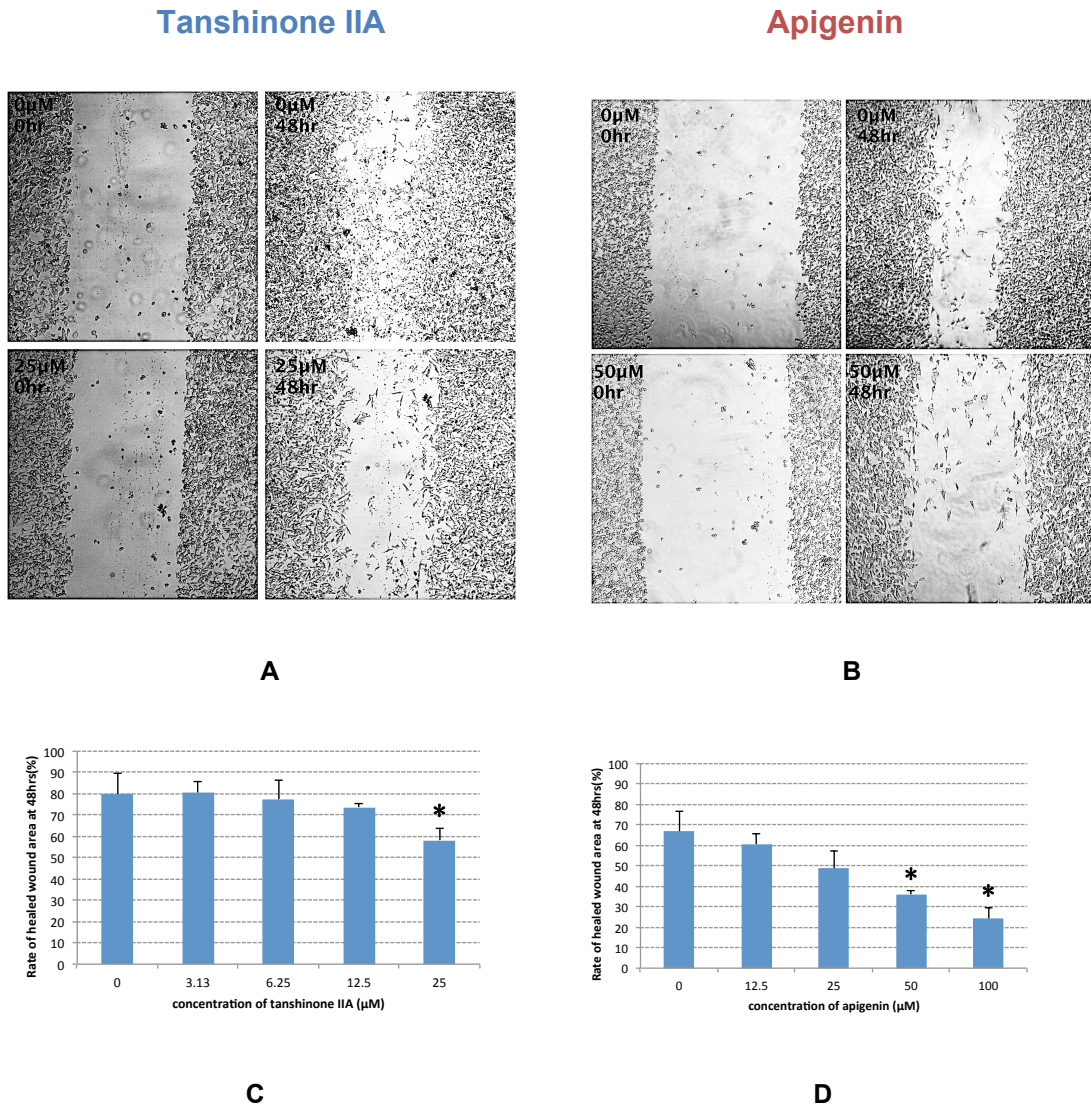
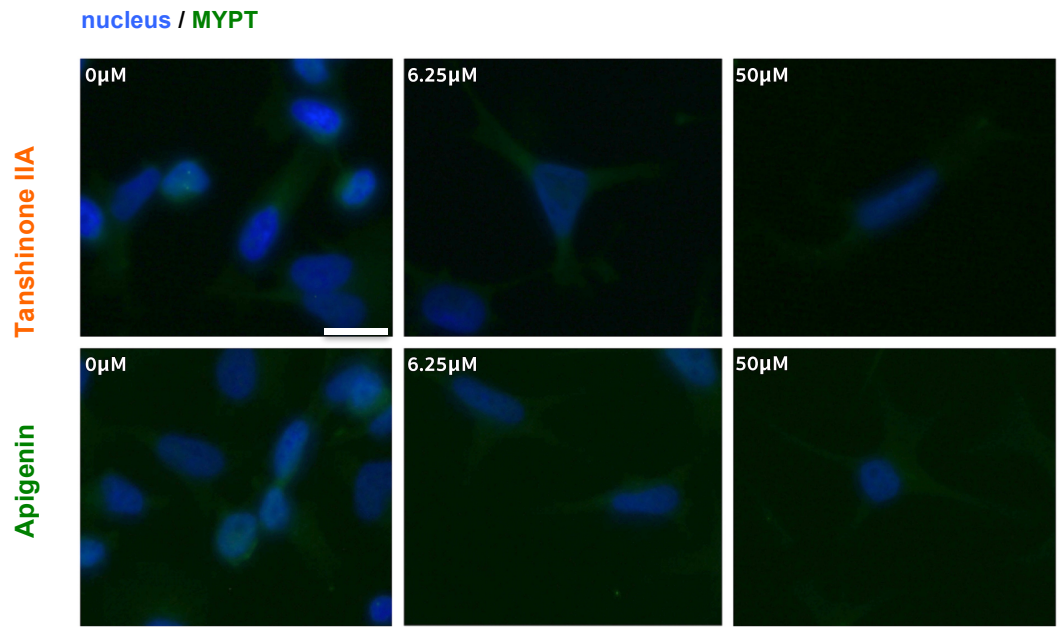


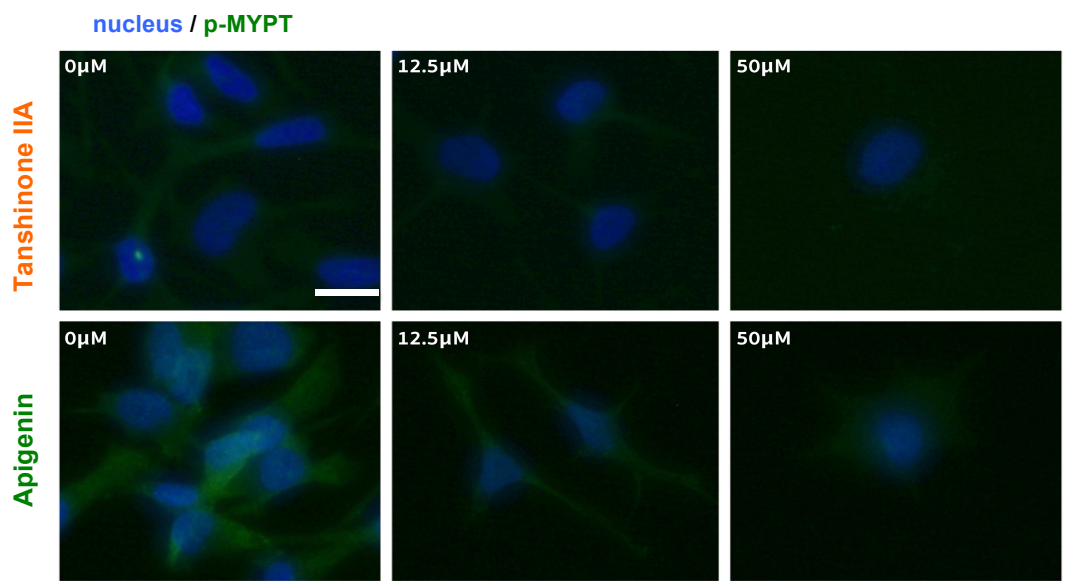
Figure 15. Scratch assay of 92.1 cells treated with tanshinone IIA (A) and apigenin (B) respectively. Phase contrast images were acquired after creating the wound in the confluent monolayer (0 hr) and at the end of the incubation period (48 hrs, Magnification: 50X). Quantifications demonstrated the significant and dose-dependent reduction in the invasion of the wound area in the cells treated with tanshinone IIA (C) or apigenin (D) versus control groups. Data represent the mean \pm SEM of three independent experiments. * $P < 0.05$ compared to 0 μM tanshinone IIA or apigenin.

MYPT1 and p-MYPT1 immunostaining: Rho-Kinase activity in response to tanshinone IIA / apigenin

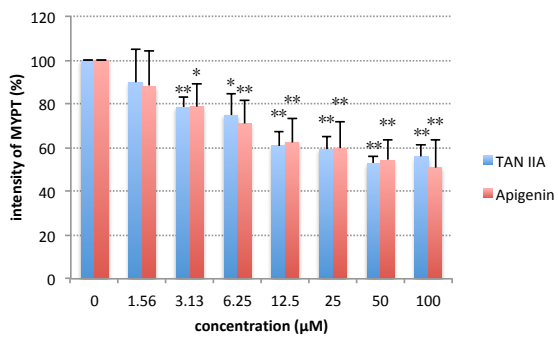
Activity of Rho-kinase was assessed by determining the levels of the myosin phosphatase target subunit 1 (MYPT1), one of the major substrates of Rho-kinase, and its phosphorylation at threonine 696 (p-MYPT1), the major Rho-kinase-dependent phosphorylation site of this protein. A dose-dependent decrease of MYPT expression was observed at the concentration of 3.13 μ M tanshinone IIA or apigenin onwards. Likewise, the intensity of the p-MYPT1 immunostaining exhibited a significant and dose-dependent decline with both flavonoids at the end of 3 days. The intensity ratio of p-MYPT to MYPT rose in a dose-dependent manner in response to the flavonoids, however, this effect did not reach statistical significance. Our results therefore demonstrate that both tanshinone IIA and apigenin might interfere with the Rho-kinase signalling by decreasing the levels of the major Rho-kinase target MYPT1 and its phosphorylation at threonine 696 after 3 days, without significantly affecting the ratio of the phosphorylated to the total protein. (*Figure 16*)



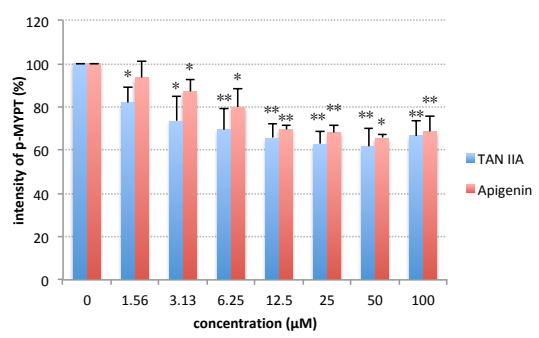
A



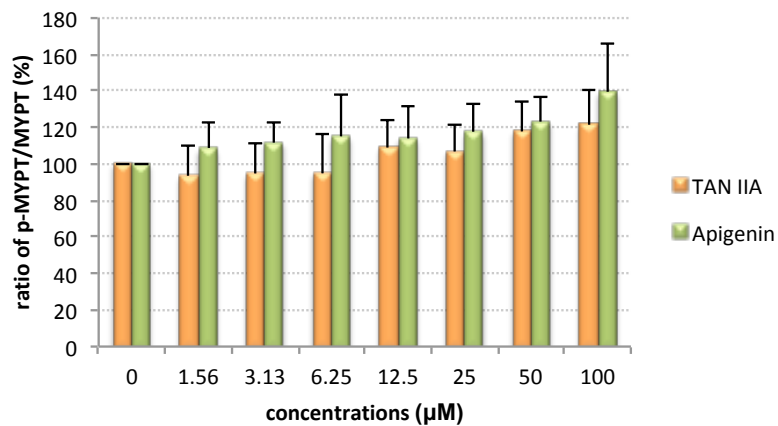
B



C



D

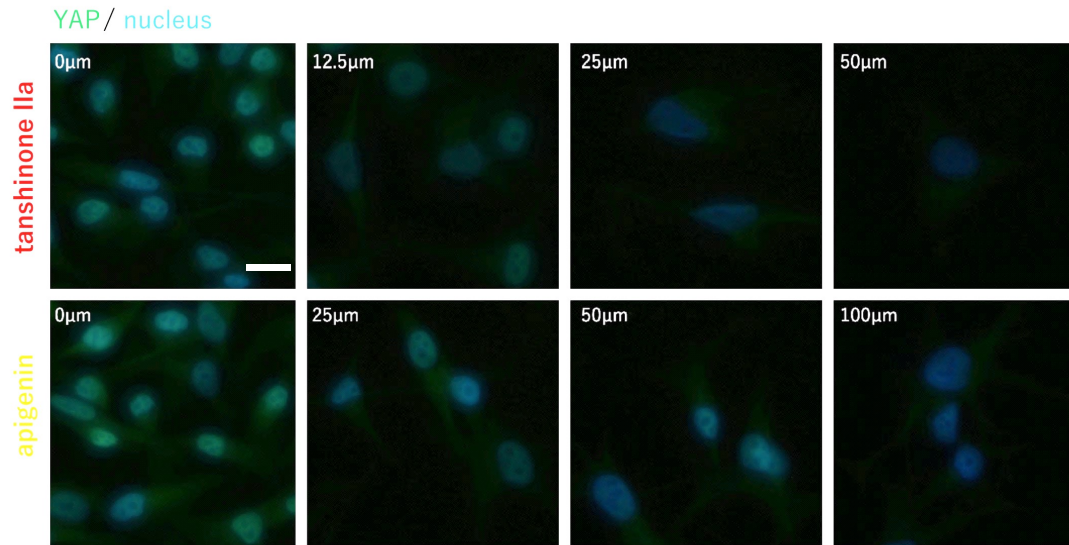


E

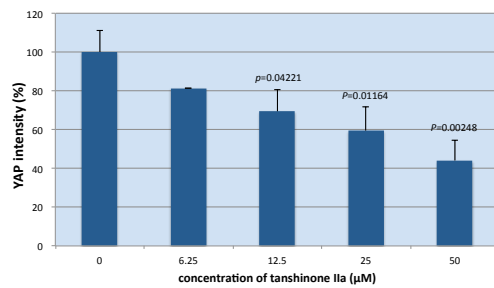
Figure 16. Significant dose-dependent reductions in the expression of myosin phosphatase (A/C) and its phosphorylation (p-MYPT) (B/D) in 92.1 cells incubated with tanshinone IIA or apigenin for 72 hours. Scale bar=25 μm. Diagrams of data represent the mean ± SEM of n=3 independent experiments. Histogram (E) presents the ratio of p-MYPT and MYPT with no statistical significance compared to the control groups. *P* values compared to control group. **P*<0.05 ***P*<0.01

Expression of YAP-1 after the treatment with tanshinone IIA and apigenin

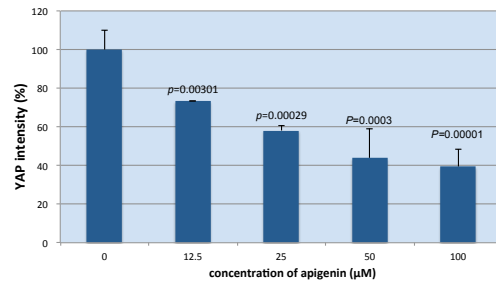
The expression pattern of the transcriptional co-activator YAP-1 in 92.1 cells was evaluated by fluorescence immunocytochemistry. Untreated cells exhibited a strong expression of this protein in the nuclear region whereas the incubation with tanshinone IIA or apigenin led to a significant decrease in YAP-1 levels in a dose-dependent manner. (Figure 17)



A



B



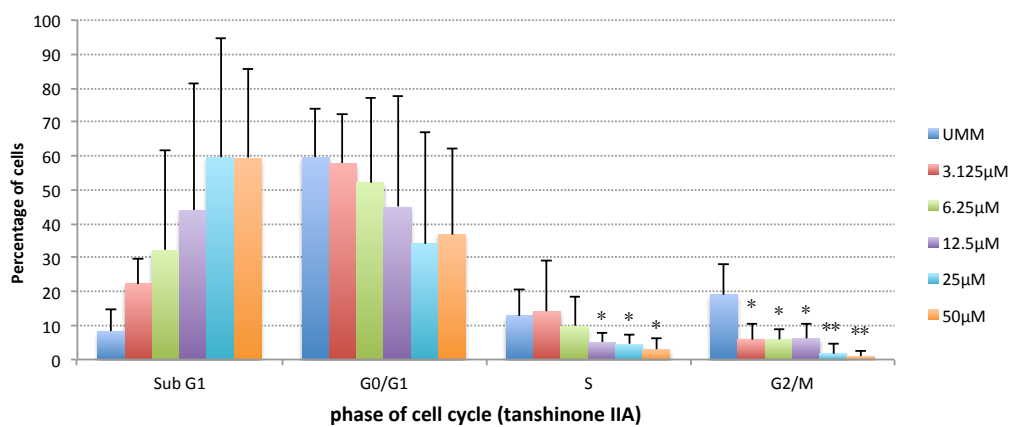
C

Figure 17. YAP-1 immunostaining of 92.1 cells under the treatment with tanshinone IIA or apigenin for 72 hours. (A) Merged fluorescence images demonstrate that the expression of YAP-1 could be significantly suppressed by tanshinone IIA or apigenin in a dose-dependent manner. Scale bar=25 μm. Histograms illustrate a significant and dose-dependent decrease in the intensity of nuclear YAP-1 expression in response to tanshinone IIA (B) or apigenin (C) compared to the control. *P* values compared to the control group. Diagrams of data represent the mean ± SEM of n=3 independent experiments.

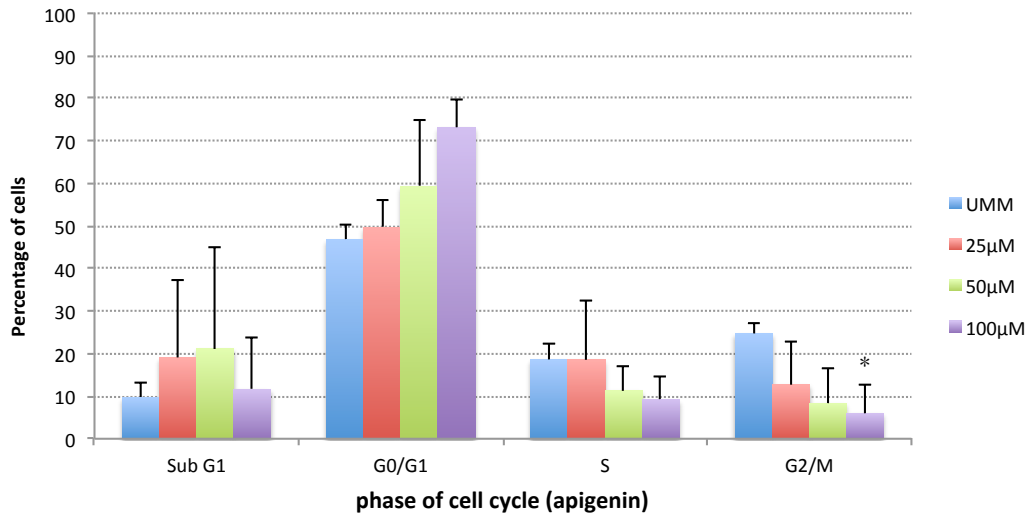
Induction of cell cycle arrest by tanshinone IIA and apigenin

Different cell cycle phases were determined by measuring the integrated density of the DNA binding dye DAPI in the fluorescence microscopy images of the 92.1 cells treated with or without the flavonoids for 3 days. The cell cycle phases are defined as the Sub G1 stage (cells with DNA loss), G0/G1 (Quiescent / Gap 1) stage, S (DNA synthesis) stage, and G2/M (Gap 2 / Mitosis) stage. The thresholds for these cell cycle phases were determined by plotting the integrated density values of untreated cells against the number of cells having such values.

Histograms demonstrated a distributional change in the percentage of cells that could be assigned to the distinct cell cycle phases. Generally, both flavonoids resulted in a significant and dose-dependent decrease in the percentage of cells committed to proliferation (S and G2/M phases). With increasing concentrations, tanshinone IIA led to the accumulation of 92.1 cells in the Sub G1 phase, while apigenin induced UM cell cycle arrest mainly in the G0/G1 phase. (Figure 18)



A



B

Figure 18. Dose-dependent cell-cycle arrest in response to tanshinone IIA and apigenin. The thresholds for different cell cycle stages were defined by plotting the number of untreated cells (in normal medium, UMM) against their DNA-content (N), which was measured as the integrated density of the DNA-binding dye DAPI (Sub G1: Cells with less than 2N; G0/G1: 2N (diploid cells, containing two copies of each chromosome); S: more than 2N, less than 4N; G2/M: 4N or more). Histograms illustrated that tanshinone IIA promoted an increase in the percentage of cells in the Sub G1 stage (A: n=6 independent tests), whereas cell cycle arrest was more likely to present at the G0/G1 stage when they were incubated with apigenin (B: n=4 independent tests). * $P < 0.05$ compared to the untreated group.

DISCUSSION

The biggest challenge in the management of UM is to find an effective treatment to prevent the metastasis and improve the prognosis. Depending on the different developmental stages of UM, radiotherapy and surgical resection are the main conventional therapeutic principles for UM patients. Unfortunately none of these therapies can effectively prevent the progression of the metastatic disease, but result in physical and psychological burdens on patients in return.

Interestingly, certain natural substances could exert chemopreventive and anti-tumor effects in current preclinical research (17,36). In the Zutphen Elderly Study, five flavonoids (quercetin, kaempferol, myricetin, apigenin and luteolin) were administered daily to 738 individuals, who were aged 65-84 years old and had no tumor history. Final evaluations after the follow-up period of 5 years showed that the high intake of these flavonoids from vegetables and fruits was inversely associated with the risk of cancer development (40). Several cancers, for example breast cancer, have a lower incidence in Asia than in western countries (29). This may be attributed to the typical Asian dietary regimens that are customarily rich in flavonoid-containing plants. Tanshinone IIA and apigenin, the test substances in our study, have been reported to possess various beneficial biological properties, such as anti-carcinogenic, anti-oxidant, anti-mutagenic, anti-proliferative, and anti-inflammatory effects (12,34,62,78,91). In addition, in comparison with other structurally related flavonoids, apigenin has gained a particular attraction as a potential antitumor reagent, due to its lower intrinsic toxicity and beneficial effects

on normal cells (34).

However, the possible anti-metastatic effects of flavonoids and the underlying mechanisms have not been fully elucidated yet in UM cells. Our study aimed to evaluate the effects of tanshinone IIA and apigenin on different metastatic aspects of the 92.1 UM cells, such as cell viability, proliferation, and migration. Moreover, the possible molecular targets and signaling pathways that were affected by these two flavonoids were investigated as well, with particular attention to the Rho-kinase dependent events.

UM cell viability in response to tanshinone IIA and apigenin

The analysis of cell viability was performed based on the principle of intracellular enzymatic activities in viable cells and intact plasma membranes. In our study, we first applied the MTT assay to determine the metabolic activity of the 92.1 cells. Additionally, the percentage of damaged cells after the treatment with tanshinone IIA or apigenin was detected through the measurement of EthD-1 fluorescent staining. EthD-1 is a high-affinity nucleic acid stain, which is applied as a cell-impermeant viability indicator. After entering the cells with damaged membrane, it binds to nucleic acids, which results in an enhancement of its fluorescence emission.

After the treatment with tanshinone IIA or apigenin, both assays demonstrated a significant and dose-dependent decrease in the viability of 92.1 cells in our study. The IC₅₀, as assessed by the MTT test, was 6.48 μ M for tanshinone IIA and 66.58

μM for apigenin. The results of apigenin treatment were in accordance with the findings of an earlier study (37), which demonstrated a significant reduction of metabolically active cutaneous melanoma cells incubated with 50 μM apigenin, but no difference in cell viability at lower concentrations. Likewise, the treatment with Tanshinone IIA resulted in the upregulation of apoptotic proteins in certain tumor cells, such as the human gastric cancer, cervical cancer, and hepatoma cells (43,94). Our results on UM cells therefore provided further support to the tumor-suppressing effect of these flavonoids.

Tanshinone IIA and apigenin-dependent cell cycle arrest in UM cells

Cell cycle is a complex biological process involving the duplication of chromosomes and resulting in the division of a cell into two daughter cells. Generally, the majority of the cells remain at the G₀/G₁ phase without apparent activity related to cell division. The G₀ phase is a quiescent state, at which the cells carry out their normal, differentiated functions without actively preparing for division. At the first growth (G₁) phase, the cells start the production of building blocks and organelles. These biosynthetic activities increase further in the cells committed to proliferation. The replication of DNA during the following synthesis (S) phase leads to a gradual increase in the total DNA intensity. Cells that manage to complete the S phase proceed further to growth and enter the G₂/M (mitotic) phase, at which the DNA content is two times more than the cells at the G₀/G₁ phase. In the mitotic (M) phase, the cell equally separates the duplicated genetic material into two poles and

divides its cytoplasm (cytokinesis), which results in the formation of two daughter cells and completion of the cell cycle. Interestingly, some cells can present with a significantly lower DNA level than the cells in the G₀/G₁ phase. Such cells in the sub-G₁ stage are considered to be damaged cells. To avoid any error during the complicated cell cycle process, there are three main checkpoints: the G₁/S checkpoint, the G₂/M checkpoint and the metaphase (mitotic) checkpoint, which prevent the entry of the cells into the next step of the cell cycle until certain requirements are met. However, despite these stringent controlling mechanisms, failure in the regulation of cell division can still occur, which often leads to tumor formation. On the other hand, alterations in the length of certain cell cycle phases can provide valuable information on the impairment of cell cycle progression and the efficacy of anti-cancer treatments.

Based on these principles, we evaluated the outcomes of tanshinone IIA and apigenin treatment on the percentage of UM cells in specific phases of the cell cycle. For this purpose, the nuclei of untreated and treated cells were stained with the DNA-binding fluorescent dye DAPI and the integrated density of the DAPI-staining was quantified to determine the DNA levels. Our results showed that tanshinone IIA promoted the accumulation of the 92.1 cells at the Sub-G₁ stage, whereas apigenin led to an increase in the amount of cells at the G₀/G₁ phase. These results suggested that tanshinone IIA could induce a notable degree of cell damage in the 92.1 cells, as reflected by the amount of cells in the Sub-G₁ phase, while apigenin could induce cell cycle arrest mainly in the G₀/G₁ phase.

The rearrangement of actin filaments, such as the formation of stress fibers during interphase and contractile rings during mitosis, is one of the most important events throughout the progression of cell cycle (71,54). The assembly of the actin cytoskeleton is mainly regulated by the Rho-GTPases and the RhoA/RhoC effector Rho-kinase. Accordingly, the Rho/Rho-kinase pathway was found to be playing a critical role at different steps of the cell cycle progression, particularly during the G1/S transition and cytokinesis (39,108). Interestingly, our study also demonstrated the direct effect of tanshinone IIA and apigenin on the organization of the actin cytoskeleton as well as the expression and phosphorylation of MYPT1, the major target of Rho-kinase. (Figure 13, 16) The impairment of Rho/Rho-kinase activity and the associated remodeling of the actin filaments might therefore be one of the reasons underlying the flavonoid-dependent cell cycle arrest in our study, which deserves further investigation.

The inhibitory effect of various flavonoids on the cell cycle progression of tumor cells has been well demonstrated in numerous other studies, including *in vitro*, *in vivo* and clinical trials (80). For instance, tanshinone IIA could effectively promote the cell cycle arrest of cancer cells at G0/G1, S or G2/M, depending on its concentration and the cell type (115,100). Interestingly, Zhou et al. (116) found that tanshinone IIA could arrest cancer cells before metaphase-anaphase transition during mitosis by disrupting the mitotic spindle, which is the period mainly regulated by Rho-GTPases. Unlike other chemotherapeutic drugs, such as the taxanes or vinca alkaloids, that were originally identified in plants and that cause G2/M arrest

by acting on the spindle microtubule structure, tanshinone IIA destroyed the mitotic spindle during interphase. Likewise, apigenin could increase the amount of breast cancer cells in the sub-G1 phase (60). Our results demonstrate for the first time the efficacy of tanshinone IIA and apigenin to induce cell cycle arrest in UM cells. Further studies to elucidate the molecular pathways involved in this process would provide more support to the therapeutic potential of these promising flavonoids.

Tanshinone IIA and apigenin suppress the proliferation of UM cells

Our results showed a significant reduction in the expression of the proliferation marker Ki-67 in response to tanshinone IIA at lower concentrations (12.5 and 25 μM). In contrast, apigenin had a weaker impact on UM cells at such concentrations and could exert a significant anti-proliferative effect at 50 and 100 μM . Interestingly, the inhibitory effect of tanshinone IIA on Ki67 expression weakened unexpectedly at the concentrations of 50 μM and 100 μM . Several studies have reported similar results, suggestive of the differential impact of flavonoids on tumor cells at lower and higher concentrations. For example, genistein was reported to be biphasically regulating prostate cancer cell proliferation and invasion after 72 hours *in vitro*, represented as a 1.5-fold increase at 0.5 to 1 μM concentrations and ~3.0-fold decrease at 50 μM (22). Likewise, a similar effect was observed in breast cancer cells after treatment with the soybean isoflavone daidzein (59). Since the uveal melanoma cells appeared apoptotic after the incubation with high concentration of tanshinone IIA, (Figure 13A) the weakened anti-proliferation of high concentration

of tanshinone IIA might be explained by the overestimation of the unspecific binding of antibodies due to apoptotic protein degradation at very high concentrations of the flavonoids, or the subcellular fragments produced by the disintegration of the dead cells, or the condensed apoptotic cells, which may functioned as unspecific targets leading to the contradictory results (67). However, there is currently no clear interpretation on such concentration-dependent contrasting actions of flavonoids on cancer cells.

The downregulation of Ki67 in response to tanshinone IIA was also observed in the gastric cancer cell line SGC-7901 (114). However, the signaling pathway(s) regulating this event remain unknown. As stated previously, the Rho-kinase has a well-established role in the formation of stress fibers, cell adhesion and fibronectin matrix assembly in tumor cells (48). Accordingly, the Rho-kinase inhibitors such as Y-27632 and fasudil could inhibit the growth of carcinoma cells by disrupting the F-actin dynamics and stress fiber formation (93,110). Our results also suggest that tanshinone IIA and apigenin may be interfering with the Rho/Rho-kinase signaling pathway in the 92.1 cells, as demonstrated by the changes in the actin cytoskeleton and the levels of the main Rho-kinase target MYPT. (*Figures 13,16, respectively*) Further investigation of the Rho-kinase mediated events would provide valuable insight into the molecular mechanisms underlying the anti-proliferative effect of these flavonoids.

Tanshinone IIA and apigenin suppress the motility of UM cells

During cell migration, actin microfilaments collaborate with microtubules to direct the cells to their destination by the protrusion of the leading edge, tail retraction and ECM adhesion. The Rho/mDial pathway is involved in the regulation of actin polymerization for the protrusion in the front, whereas the Rho/Rho-kinase signaling pathway controls the integrin adhesion of the tails and induces tail retraction (71). Accordingly, the treatment of skin melanoma cells with the novel Rho-kinase inhibitors CCT129254 or AT13148 could reduce cellular invasion (86). Using scanning electron microscopy, Routhier A et al. (85) also found that the treatment of UM cells with the synthetic Rho-kinase inhibitor Y-27632 resulted in an increased filopodia formation and limited lamellipodia formation.

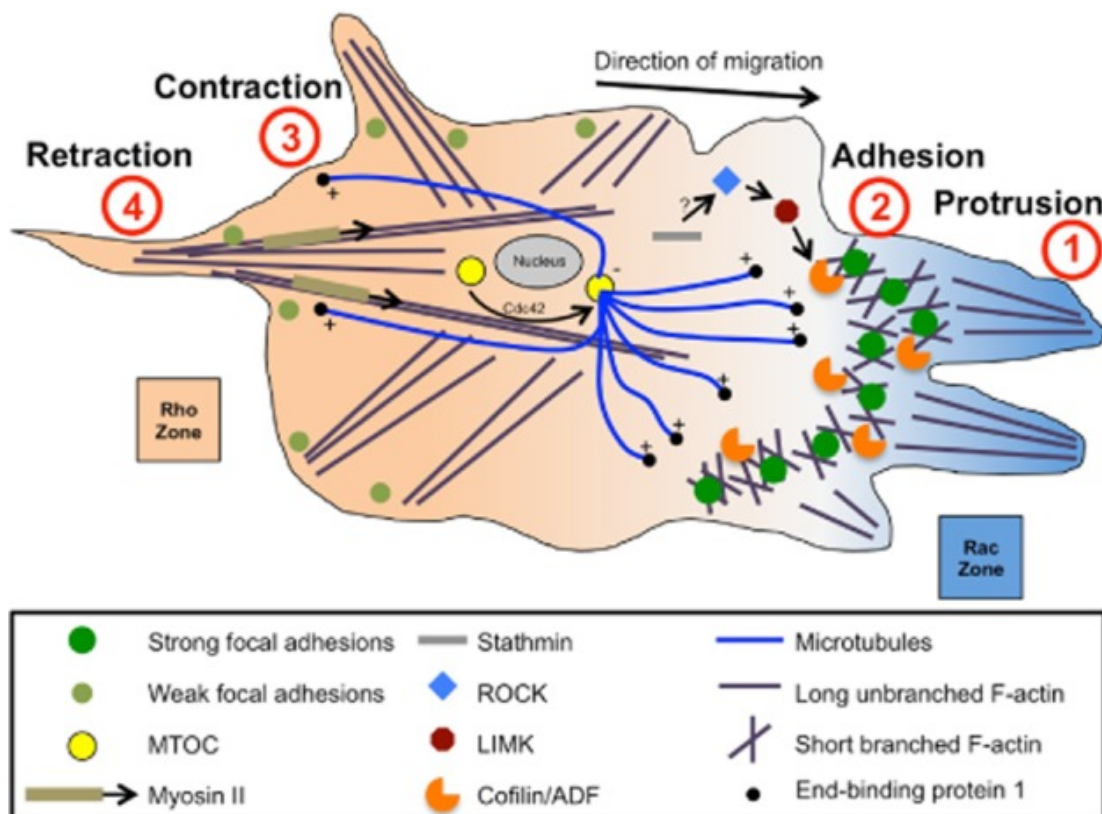


Figure 21. The four steps of cell migration and underlying rearrangement of the cytoskeleton. Cell motility is generally divided into four procedures: head protrusion, ECM adhesion, cell contraction and tail retraction. The polymerization of F-actin generates the protrusions at the leading edge, while the depolymerization of F-actin leads to the retraction of the tailing part. The actin cytoskeleton is mainly regulated by the Rho-kinase and its relevant downstream targets, such as LIMK and cofilin. (ROCK= Rho-kinase; MTOC=Microtubule organizing center) (25)

In our study, tanshinone IIA and apigenin reduced the cell motility into the scratched wounds of 92.1 UM cells monolayer in a dose-dependent manner. This is in agreement with the degradation of actin microfilaments in response to tanshinone IIA and apigenin, as indicated by the phalloidin staining. The impairment of the stress fiber formation might therefore have reduced the contractile strength of the cells, resulting in the impairment of cellular invasion.

Tanshinone IIA and Apigenin reorganized the actin microfilaments and changed the morphology of UM cells

The actin cytoskeleton is recognized as the molecular fundament implicated in numerous metastatic aspects of cancer progress, such as proliferation and motility. We therefore assessed the outcomes of flavonoid treatment on UM cell morphology by staining the actin filaments. Increasing levels of tanshinone IIA and apigenin significantly weakened the intensity of the F-actin staining in a dose-dependent manner. Interestingly, adding very high concentrations (100 μ M) of tanshinone IIA and apigenin promoted a contracted, apoptotic appearance. Cells in the intermediate concentration groups, on the other hand, exhibited a more

dendritic, and branch-like morphology, which is similar to the normal, differentiated melanocytes. This is in agreement with the observations of a former study on cutaneous melanoma cells, where the incubation with 20 μM apigenin for 1 day promoted the formation of long protrusions, whereas the higher concentrations (up to 50 μM) induced a rounded and granulated morphology (37). Interestingly, the loss of melanocytic differentiation as well as the acquisition of primitive stem-like cells are the two important features that distinguish metastatic UM from the non-metastatic tumors (36). This might suggest that the lower concentrations of the flavonoids tested in our study might reverse the de-differentiated state of malignant UM cells to normal, functional melanocytes with less metastatic potential. This may also partially explain the suppressive effects of these flavonoids in the growth and migration tests in our study.

Tanshinone IIA and apigenin exert inhibitory effects on Rho-kinase/MYPT and Rho-kinase/YAP signaling pathways

As stated previously, the best known regulators of the organization of actin cytoskeleton are the Rho-GTPases and their main downstream effector Rho-kinase (35). The most important downstream targets of Rho-kinase include the myosin light chain (MLC) and the myosin phosphatase target subunit 1 (MYPT-1) (88,102). In UM cells, phosphorylation of MYPT-1 (myosin phosphatase target subunit 1, also known as myosin binding subunit or MBS) inhibits the dephosphorylation of MLC (73,74). The phosphorylated MLC in turn catalyzes

actin-myosin filament bundling and myosin-driven contraction, therefore initiating several tumor-associated processes, such as morphological changes, cell motility, proliferation, and adhesion (81).

Our results showed that tanshinone IIA and apigenin decreased the levels of both MYPT and its phosphorylation at threonine 696, the major site targeted by Rho-kinase, in a dose-dependent manner. Interestingly, the very high concentrations of both flavonoids, which induced an apoptotic morphology, led to a gradual increase in the ratio of p-MYPT to MYPT levels, but this effect did not reach statistical significance. High concentrations of flavonoids, as mentioned above, might cause the degradation of cellular proteins in apoptotic cells, which might create unspecific binding targets for the antibodies, leading to the slight higher expression of p-MYPT over MYPT (67). This might also attribute to other involved unknown protein molecules or signaling pathways, which are worthy of further investigations.

The increased Rho-kinase activity in UM cells due to the mutations in Gαq/11 also induces the translocation of the YAP protein to the nucleus, which promotes UM cell growth (24,63,112). YAP functions as a transcriptional co-activator and presents in most proliferating cells (76,79). Normally, the level of YAP in proliferating cells remains in dynamic stability that is regulated by cellular density. When cells reach to an appropriate number, the signaling cascades that are activated by cell-cell contacts lead to the rearrangement of the actin cytoskeleton and degradation of YAP in the cytosol, which prevents further cell growth (24).

Conversely, the accumulation of unphosphorylated YAP in the nucleus would allow for its interaction with the related transcription factors and further promote the expression of proliferative genes (111). Accordingly, knocking down the mutant Gαq gene in UM cells increased the phosphorylation of YAP, decreased YAP nuclear localization, and suppressed tumor growth in an *in vivo* study (63). Moreover, YAP-deficient UMs developed significantly smaller than the controls (113). Currently, the YAP inhibitor verteporfin has been approved by the FDA (Food and Drug Administration) to be utilized in the photodynamic therapy (PDT) of eyes against abnormal blood vessel formation. However, it still has a limited use abroad due to its low solubility.

Our study demonstrated that tanshinone IIA and apigenin reduced the expression of nuclear YAP in a dose-dependent manner, possibly due to the degradation of actin microfilaments. These findings provide further support to the promising therapeutic potential of both flavonoids for the treatment of UM patients. To confirm these findings, it would be very beneficial to perform further analyses in other UM cell lines and evaluate the underlying mechanisms in the future.

A possible mechanism of the inhibitory effects of the flavonoids in our study might be related to the structural similarity of flavonoids to adenosine. (Figure 4) Adenosine and its derivatives, such as the adenosine triphosphate (ATP), adenosine diphosphate (ADP) and cyclic adenosine monophosphate (cAMP), play vital roles in biochemical processes like energy transfer, vasodilation and neuromodulation. It is also well described that tumor cells can release adenosine

due to the hypoxic environment, which induces the accumulation of extracellular adenosine. The activation of adenosine receptors by the extracellular adenosine can in turn promote the growth and development of tumors (1,51). Accordingly, the inactivation of adenosine receptors emerges as a promising therapeutic approach to suppress tumor growth (51). Interestingly, certain flavonoids have also been indicated as adenosine receptor antagonists (42,69), possibly due to the mild similarity of their structure to adenosine. (Figure 4) Flavonoids could also activate the adenosine monophosphate-activated protein kinase (AMPK), which is proposed as a major controller of cell proliferation and apoptosis (64). These aspects might bring us a new insight, that flavonoids can be utilized as potential competitors of adenosine receptors against oncogenesis and metastasis.

Moreover, the synthetic Rho-kinase inhibitors exert their effects by targeting the ATP-binding domain of these enzymes (98). As stated previously, Rho-kinase plays a substantial role in the growth and metastasis of UM cells. To date, two Rho-kinase inhibitors have been authorized for clinical application: Fasudil was approved in Japan in 1995 and is now used for preventing cerebral vasospasm as an inhibitor of actomyosin contraction (74). Ripasudil was ratified in Japan in 2014, to be applied as eye drops for improving the outflow of the intraocular aqueous humor as a therapeutic management for ocular hypertension and glaucoma (28). However, the clinical approval of these synthetic inhibitors in Europa may take many more years. On the other hand, the dietary flavonoids such as tanshinone IIA and apigenin are readily available, natural, and botanically extracted nutraceuticals.

Our results provide the first evidence that these flavonoids can interfere with many of the cellular events regulated by Rho-kinase in a certain UM cell line, such as survival, cell cycle progression, proliferation, motility, rearrangement of the actin cytoskeleton, and YAP activation. Tanshinone IIA and apigenin can therefore be considered as readily available and natural inhibitors of UM cell growth and metastasis. To further evaluate the therapeutic potential of these flavonoids, it would be invaluable to conduct *in vitro* assays on additional UM cell lines and *in vivo* experiments in the future.

SUMMARY

Uveal melanoma (UM) is the most common and potentially devastating primary intraocular malignancy in adults with an extremely high rate of metastasis and mortality. There is currently no standard treatment for metastatic UM. In this study, we evaluated the efficacy of flavonoids, tanshinone IIA (TAN IIA) and apigenin, as potential inhibitors of the metastatic activities of UM cells.

In our study, we evaluated the optimal concentration of the flavonoids, the organization of the actin cytoskeleton, cell migration, proliferation, cell viability and the cell cycle arrest of UM cells 92.1 treated with TAN IIA or apigenin at a concentration range of 1.5-100 μ M. In order to investigate the underlying molecular pathways involved, activity of Rho-kinase and YAP-1 was assessed by the immunostaining for MYPT-1, phosph-MYPT and YAP-1.

TAN IIA and apigenin led to a significant and dose-dependent reduction in the number of metabolically active cells and actin microfilaments staining, and a dose-dependent increase in the intake of EthD-1 in the treated groups compared to the control ($p < 0.05$). TAN IIA or apigenin inhibited the migration of cells after treatment for two days ($p < 0.05$) and declined the upregulation of the Ki67. Flavonoids induced significant reductions of the expression of MYPT-1, p-MYPT and YAP-1 in a dose-dependent manner.

Our study showed promising inhibitory effects of TAN IIA and apigenin on the metastatic activities of the 92.1 cells. Flavonoids might be considered as natural, efficient pharmaceutical therapies with lower side effects for the UM patients.

Zusammenfassung

Das uveale Melanom ist die häufigste primär intraokuläre maligne Erkrankung des Erwachsenen mit einer sehr hohen Metastasierungsrate und Letalität. Bei 50% der Patienten treten innerhalb von fünf Jahren Metastasen auf, daher ist die derzeitige Therapie des primär uvealen Melanoms nicht mit einem signifikanten Überlebensvorteil verbunden. So beträgt die durchschnittliche Überlebenszeit nachzeitigem Stand noch lediglich 12-14 Monate. Eine effektive Prävention der Metastasierung ist demnach das oberste Ziel in der Behandlung von Patienten mit UM.

Molekulare Mechanismen, welche der Entwicklung des UM zugrunde liegen, müssen noch weiter erforscht werden. Unter anderem ist bekannt, dass das UM durch Mutationen in den GNAQ oder GNA11 Genen, die für die G-Protein-alpha-Untereinheiten Gq und G11 kodieren, ausgelöst wird. Diese Mutationen führen zur Konversion dieser Signalproteine in eine konstitutiv aktive Form. Kürzlich veröffentlichte Untersuchungen konnten aufzeigen, dass die durch den Rho/Rho-Kinase Signalweg ausgelöste erhöhte Aktivität des transkriptionellen Co-Aktivators *yes-associated protein-1* (YAP-1) Wachstum und Entwicklung von UM-Zellen begünstigt. Somit stellt dieses Signal ein potentielles Target für neue Therapien dar. Vielversprechende Studien wiesen nach, dass synthetische Rho-Kinase-Inhibitoren sowohl Überleben, als auch Motilität und Proliferation von kultivierten UM-Zellen verhindern konnten. Jedoch existieren zur Zeit keine Studien, die speziell auf die Nutzbarkeit natürlicher Inhibitoren mit Wirkung auf die

metastasierenden Eigenschaften von UM-Zellen ausgelegt sind.

Flavinoide sind die am weitesten verbreiteten bioaktiven phytochemischen Verbindungen und finden sich in Kräutern und anderer pflanzlicher Nahrung. Es ist bereits nachgewiesen, dass Flavinoide vorteilhafte biologische Auswirkungen auf die Metastasierung verschiedener Tumorzellen haben. Unser Interesse galt zwei Flavinoiden, Transhinone IIA und Apigenin, im Hinblick auf ihre Wirkung als potentielle Inhibitoren von Überleben und Metastasierung von UM-Zellen.

Im Rahmen unserer Studie wurden Zellen des Stammes 92.1 mit TAN IIA oder Apigenin in den Konzentrationen 1,5 bis 100 μM behandelt. Die optimale Konzentration wurde mittels eines MTT-Assays ermittelt. Die Organisation des Aktiv-Zytoskeletts wurde mit einer Phalloidin-Färbung analysiert. Ein scratch-Assay untersuchte die Zell-Migration. Die Proliferation der Zellen wurde mithilfe einer Ki67-Immunfärbung analysiert. Um die zugrundeliegenden molekularen Signalwege zu analysieren, wurden die Aktivitäten der Rho-Kinase und YAP-1 mittels Immunfärbung von MYPT-1 (*myosin phosphatase target subunit-1*), phospho-MYPT-1 (p-MYPT-1) und YAP-1 bestimmt. Der Zellzyklus-Arrest wurde bestimmt, indem die Intensität des DNA-bindenden Farbstoffs DAPI gemessen wurde.

Unsere Ergebnisse weisen nach, dass TAN IIA und Apigenin zu einer signifikanten Reduktion von metabolisch aktiven 92.1 Zellen geführt haben. Desweiteren führte eine Behandlung der Zellen mit 50 μM TAN oder Apigenin zu einer signifikant dosisabhängigen Reduktion der F-Aktin-Färbung. Dies weist auf eine Beeinträchtigung des Zytoskeletts hin. Außerdem wirkte sich TAN verlängernd

auf die Protrusionen aus und führte zu morphologischen Veränderungen der 92.1-Zellen im Vergleich zur epitheloidzellartigen Kontrollgruppe. Die Zellmigration in Richtung des Wundbereiches wurde offensichtlich durch mittel bis hohe Konzentrationen von TAN IIA und Apigenin verhindert. Die Proliferation wurde signifikant durch TAN IIA reduziert, wohingegen Apigenin im Vergleich eine schwächere Auswirkung aufwies. Eine Verminderung der Zellviabilität durch TAN IIA und Apigenin könnte durch eine Schädigung der Plasmamembran erklärt werden. Dies könnte mit einer Veränderung der Rho-Kinase Aktivität einhergehen, welche durch eine reduzierte Expression von MYPT-1, p-MYPT-1 und YAP-1 durch TAN IIA und Apigenin ersichtlich ist. Die Analysen des Zellzyklus deuteten auf eine Störung in der Sub-G1-Phase durch TAN hin; Apigenin hingegen führte zu einem Zellzyklus-Arrest in der G0/G1-Phase. Damit verhindert Apigenin die DNA-Replikation und Teilung.

Unsere Ergebnisse zeigen vielversprechende inhibitorische Effekte von 92.1-UM-Zellen. Somit könnten Flavonoide für die Entwicklung von natürlichen, effizienten und sofort verfügbaren pharmazeutischen Therapien mit geringeren Nebenwirkungen für UM Patienten in Betracht gezogen werden.

REFERENCES

1. Akio Ohta: A Metabolic Immune Checkpoint: Adenosine in Tumor Microenvironment. *Front Immunol* 7: 109; 2016
2. Amin ARMR, Karpowicz PA, Carey TE, et al: Evasion of anti-growth signaling: A key step in tumorigenesis and potential target for treatment and prophylaxis by natural compounds. *Semin Cancer Biol* 35: 55-77; 2015
3. Amin ARMR, Kucuk O, Khuri FR, et al: Perspectives for cancer prevention with natural compounds. *J Clin Oncol* 27: 2712–2725; 2009
4. Augsburger JJ, Corrêa ZM, Shaikh AH, et al: Effectiveness of treatments for metastatic uveal melanoma. *Am J Ophthalmol* 148: 119–127; 2009
5. Barker CA, Francis JH, Cohen GN, et al: (106)Ru plaque brachytherapy for uveal melanoma: factors associated with local tumor recurrence. *Brachytherapy* 13: 584-90; 2014
6. Berg K, Hansen MB, Nielsen SE, et al: A new sensitive bioassay for precise quantification of interferon activity as measured via the mitochondrial dehydrogenase function in cells (MTT method). *APMIS* 98: 156-162; 1990
7. Blum ES, Yang J, Komatsubara KM, et al: Clinical Management of Uveal and Conjunctival Melanoma. *Oncology (Williston Park)* 30: 29-32, 34-43; 2016
8. Bowling B. Kanski's Clinical Ophthalmology. In: Bowling B (Hrsg.): Kanski's Clinical Ophthalmology. 8. Edition., 488, Saunders Ltd., 2015
9. Carbone M, Ferris LK, Baumann F, et al: BAP1 cancer syndrome: malignant mesothelioma, uveal and cutaneous melanoma, and MBAITs. *J Transl Med* 10:

179; 2012

10. Carvajal RD, Schwartz GK, Tezel T, et al: Metastatic disease from uveal melanoma: treatment options and future prospects. *Br J Ophthalmol* 101: 38–44; 2017
11. Chattopadhyay C, Kim DW, Gombos DS, et al: Uveal melanoma: From diagnosis to treatment and the science in between. *Cancer* 122: 2299-2312; 2016
12. Chen X, Guo J, Bao J, et al: The anticancer properties of *Salvia miltiorrhiza* Bunge (Danshen): a systematic review. *Med Res Rev* 34: 768-794; 2014
13. Chien JL, Sioufi K, Surakiatchanukul T, et al: Choroidal nevus: a review of prevalence, features, genetics, risks, and outcomes. *Curr Opin Ophthalmol* 28: 228-237; 2017
14. Chin VT, Nagrial AM, Chou A, et al: Rho-associated kinase signalling and the cancer microenvironment: novel biological implications and therapeutic opportunities. *Expert Rev Mol Med* 17: e17; 2015
15. Collaborative Ocular Melanoma Study Group: The COMS randomized trial of iodine 125 brachytherapy for choroidal melanoma: V. Twelve-year mortality rates and prognostic factors. *Arch Ophthalmol* 124: 1684–1693; 2006
16. Dall'Acqua S: Natural products as antimitotic agents. *Curr Top Med Chem* 14: 2272–2285; 2014
17. Daniels AB, Lee JE, MacConaill LE, et al: High throughput mass spectrometry-based mutation profiling of primary uveal melanoma. *Invest*

Ophthalmol Vis Sci 53: 6991-6996; 2012

18. De Waard-Siebinga I, Blom DJ, Griffioen M, et al: Establishment and characterization of an uveal-melanoma cell line. *Int J Cancer* 62: 155-161; 1995
19. Diener-West M, Earle JD, Fine SL, et al: The COMS randomized trial of iodine 125 brachytherapy for choroidal melanoma, III: initial mortality findings. COMS Report No. 18. *Arch Ophthalmol* 119: 969–982; 2001
20. Diener-West M, Hawkins BS, Markowitz JA, et al: A review of mortality from choroidal melanoma. II. A meta-analysis of 5-year mortality rates following enucleation, 1966 through 1988. *Arch Ophthalmol* 110: 245-250; 1992
21. Diener-West M, Reynolds SM, Agugliaro DJ, et al: Development of metastatic disease after enrollment in the COMS trials for treatment of choroidal melanoma: Collaborative Ocular Melanoma Study Group Report No 26. *Arch Ophthalmol* 123:1639–1643; 2005
22. El Touny LH, Banerjee PP: Identification of a biphasic role for genistein in the regulation of prostate cancer growth and metastasis. *Cancer Res* 69: 3695-3703; 2009
23. Erie JC: Uveal melanoma research and treatment at Mayo Clinic. *Mayo Clinic Ophthalmology Update* 1: 1-4; 2011
24. Feng X, Degese MS, Iglesias-Bartolome R, et al: Hippo-independent activation of YAP by the GNAQ uveal melanoma oncogene through a trio-regulated Rho GTPase signaling circuitry. *Cancer Cell* 25: 831-845; 2014

25. Fife CM, McCarroll JA, and Kavallaris M: Movers and shakers: cell cytoskeleton in cancer metastasis. *British Journal of Pharmacology* 171: 5507–5523; 2014
26. Francis JH, Shoushtarl AN, Barker CA, et al: Uveal melanoma: diagnosis, prognosis and current treatments for primary and metastatic disease. *The melanoma letter* fall 34; No. 3; 2016
27. Fronza M, Murillo R, Ślusarczyk S, et al: In vitro cytotoxic activity of abietane diterpenes from *Peltodon longipes* as well as *Salvia miltiorrhiza* and *Salvia sahendica*. *Bioorg Med Chem* 19: 4876–4881; 2011
28. Garnock-Jones KP: Ripasudil: first global approval. *Drugs* 74: 2211-2215; 2014
29. Gray GE, Pike MC, Henderson BE: Breast-cancer incidence and mortality rates in different countries in relation to known risk factors and dietary practices. *Br J Cancer* 39: 1-7; 1979
30. Griewank KG, Yu X, Khalili J, et al: Genetic and molecular characterization of uveal melanoma cell lines. *Pigment Cell Melanoma Res* 25:182-187; 2012
31. Grisanti S, Tura A: Uveal Melanoma [Internet]. In: Grisanti S, Tura A, Scott JF, Gerstenblith MR (Hrsg.): *Noncutaneous Melanoma*. 1-18, Codon, Brisbane, 2018
32. Guan R, Xu X, Chen M, et al: Advances in the studies of roles of Rho/Rho-kinase in diseases and the development of its inhibitors. *European Journal of Medicinal Chemistry* 70: 613-622; 2013

33. Gullett NP, Ruhul Amin AR, Bayraktar S, et al: Cancer prevention with natural compounds. *Semin Oncol* 37: 258–281; 2010
34. Gupta S, Afaq F, Mukhtar H: Selective growth-inhibitory, cell-cycle deregulatory and apoptotic response of apigenin in normal versus human prostate carcinoma cells. *Biochem Biophys Res Commun* 287: 914-920; 2001
35. Hall A: The cytoskeleton and cancer. *Cancer Metastasis Rev* 28: 5-14; 2009
36. Harbour JW, Chao DL: A molecular revolution in uveal melanoma: implications for patient care and targeted therapy. *Ophthalmology* 121: 1281-1288; 2014
37. Hasnat MA, Pervin M, Lim JH, et al: Apigenin attenuates melanoma cell migration by inducing anoikis through integrin and focal adhesion kinase inhibition. *Molecules* 20: 21157–21166; 2015
38. Heiss C, Keen CL and Kelm M: Flavanols and cardiovascular disease prevention. *Eur Heart J* 31: 2583-2592; 2010
39. Heng YW, Koh CG: Actin cytoskeleton dynamics and the cell division cycle. *Int J Biochem Cell Biol* 42: 1622-1633; 2010
40. Hertog MG, Feskens EJ, Hollman PC, et al: Dietary flavonoids and cancer risk in the Zutphen Elderly Study. *Nutr Cance* 22: 175-184; 1994
41. Hu DN, Yu GP, McCormick SA, et al: Population-based incidence of uveal melanoma in various races and ethnic groups. *Am J Ophthalmol* 140: 612-617; 2005
42. Jacobson KA, Moro S, Manthey JA, et al: Interactions of flavones and other phytochemicals with adenosine receptors. *Adv Exp Med Biol* 505: 163-171;

2002

43. Jeon YJ, Kim JS, Hwang GH, et al: Inhibition of cytochrome P450 2J2 by tanshinone IIA induces apoptotic cell death in hepatocellular carcinoma HepG2 cells. *Eur J Pharmacol* 764: 480-488; 2015
44. Kaliki S, Shields CL, Shields JA: Uveal melanoma: Estimating prognosis. *Indian J Ophthalmol* 63: 93–102; 2015
45. Keunen J, Korver J, Oosterhuis J: Transpupillary thermotherapy of choroidal melanoma with or without brachytherapy: a dilemma. *Br J Ophthalmol* 83: 987-988; 1999
46. Kilic E, van Gils W, Lodder E, et al: Clinical and cytogenetic analyses in uveal melanoma. *Invest Ophthalmol Vis Sci* 47: 3703-3707; 2006
47. Kim SY, Moon TC, Chang HW, et al: Effects of tanshinone I isolated from *Salvia miltiorrhiza bunge* on arachidonic acid metabolism and in vivo inflammatory responses. *Phytother Res* 16: 616–620; 2002
48. Knowles LM, Gurski LA, Maranchie JK, et al: Fibronectin matrix formation is a prerequisite for colonization of kidney tumor cells in fibrin. *J Cancer* 6: 98–104; 2015
49. Krohn J, Monge OE, Skorpen TN, et al: Posterior uveal melanoma treated with I-125 brachytherapy or primary enucleation. *Eye (Lond)* 22: 1398-1403; 2008
50. Kujala E , Mäkitie T, Kivelä T: Very long-term prognosis of patients with malignant uveal melanoma. *Invest Ophthalmol Vis Sci* 44: 4651-4659; 2003
51. Kumar V: Adenosine as an endogenous immunoregulator in cancer

- pathogenesis: where to go? *Purinergic Signal* 9: 145–165; 2013
52. Kuo PK, Puliafito CA, Wang KM, et al: Uveal melanoma in China. *Int Ophthalmol Clin* 22: 57-71;1982
53. Lam BY, Lo AC, Sun X, et al: Neuroprotective effects of tanshinones in transient focal cerebral ischemia in mice. *Phytomedicine* 10: 286–291; 2003
54. Lee K, Song K: Actin dysfunction activates ERK1/2 and delays entry into mitosis in mammalian cells. *Cell Cycle* 6: 1487-1495; 2007
55. Li G, Shan C, Liu L, et al: Tanshinone IIA Inhibits HIF-1 α and VEGF Expression in Breast Cancer Cells via mTOR/p70S6K/RPS6/4E-BP1 Signaling Pathway. *PLoS One* 10:e0117440; 2015
56. Li HW, Zou TB, Jia Q, et al: Anticancer effects of morin-7-sulphate sodium, a flavonoid derivative, in mouse melanoma cells. *Biomedicine Pharmacotherapy* 84: 909–916; 2016
57. Li W, Sun W, Yang C, et al: Tanshinone II a protects against lipopolysaccharides-induced endothelial cell injury via Rho/Rho kinase pathway. *Chin J Integr Med* 20: 216-223; 2014
58. Liao JK, Seto M, Noma K: Rho kinase (ROCK) inhibitors. *J Cardiovasc Pharmacol* 50: 17–24; 2007
59. Limer JL, Parkes AT, Speirs V: Differential response to phytoestrogens in endocrine sensitive and resistant breast cancer cells in vitro. *Int J Cancer* 119: 515–521; 2006
60. Lin CH, Chang CY, Lee KR, et al: Flavones inhibit breast cancer proliferation

- through the Akt/FOXO3a signaling pathway. *BMC Cancer* 15: 958-970; 2015
61. Liu-Smith F, Meyskens FL: Molecular mechanisms of flavonoids in melanin synthesis and the potential for the prevention and treatment of melanoma. *Mol Nutr Food Res* 60: 1264–1274; 2016
62. Long X, Zhang J, Zhang Y, et al: Nano-LC-MS/MS based proteomics of hepatocellular carcinoma cells compared to Chang liver cells and tanshinone IIA induction. *Mol Biosyst* 7: 1728-1741; 2011
63. Lyubasyuk V, Ouyang H, Yu FX, et al: YAP inhibition blocks uveal melanogenesis driven by GNAQ or GNA11 mutations. *Mol Cell Oncol* 2:e970957; 2014
64. Marín-Aguilar F, Pavillard LE, Giampieri F, et al: Adenosine Monophosphate (AMP)-Activated Protein Kinase: A New Target for Nutraceutical Compounds. *Int J Mol Sci* 18: 288; 2017
65. Mashayekhi A, Tuncer S, Shields CL, et al: Tumor-related lipid exudation after plaque radiotherapy of choroidal melanoma: the role of Bruch's membrane rupture. *Ophthalmology* 117: 1013-1023; 2010
66. Matsuoka T, Yashiro M: Rho/ROCK signaling in motility and metastasis of gastric cancer. *World J Gastroenterol* 20: 13756-13766; 2014
67. Mattes MJ: Apoptosis assays with lymphoma cell lines: problems and pitfalls. *Br J Cancer* 96: 928–936; 2007
68. Mishra KK, Quivey JM, Daftari IK, et al: Long-term results of the UCSF-LBNL randomized trial: Charged particle with helium ion vs. Iodine-125 plaque

- therapy for choroidal and ciliary body melanoma. *Int J Radiat Oncol Biol Phys* 92: 376–383; 2015
69. Moro S, van Rhee AM, Sanders LH, et al: Flavonoid derivatives as adenosine receptor antagonists: a comparison of the hypothetical receptor binding site based on a comparative molecular field analysis model. *J Med Chem* 41: 46-52; 1998
70. Munagala R, Aqil F, Jeyabalan J, et al: Tanshinone IIA inhibits viral oncogene expression leading to apoptosis and inhibition of cervical cancer. *Cancer Lett* 356: 536–546; 2015
71. Narumiya S, Tanji M, Ishizaki T: Rho signaling, ROCK and mDia1, in transformation, metastasis and invasion. *Cancer Metastasis Rev* 28: 65-76; 2009
72. Neuhouser ML: Dietary flavonoids and cancer risk: evidence from human population studies. *Nutr Cancer* 50: 1-7; 2004
73. Olson MF, Sahai E: The actin cytoskeleton in cancer cell motility. *Clin Exp Metastasis* 26: 273–287; 2009
74. Olson MF: Applications for ROCK kinase inhibition. *Curr Opin Cell Biol* 20:242–248; 2008
75. Onken MD, Worley LA, Long MD, et al: Oncogenic mutations in GNAQ occur early in uveal melanoma. *Invest Ophthalmol Vis Sci* 49: 5230–5234; 2008
76. Pan D: The hippo signaling pathway in development and cancer. *Dev Cell* 19: 491-505; 2010

77. Pan Y, Diddie K, Lim JI: Primary transpupillary thermotherapy for small choroidal melanomas. *Br J Ophthalmol* 92: 747-750; 2008
78. Patel D, Shukla S, Gupta S: Apigenin and cancer chemoprevention: progress, potential and promise (review). *Int J Oncol* 30: 233-245; 2007
79. Ramos A, Camargo FD: The Hippo signaling pathway and stem cell biology. *Trends Cell Biol* 22: 339-346; 2012
80. Rao CV, Kurkjian CD, Yamada HY: Mitosis-targeting natural products for cancer prevention and therapy. *Curr Drug Targets* 13: 1820-1830; 2012
81. Rath N and Olson MF: Rho-associated kinases in tumorigenesis: re-considering ROCK inhibition for cancer therapy. *EMBO Rep* 13: 900-908; 2012
82. Ren B, Zhang YX, Zhou HX, et al: Tanshinone IIA prevents the loss of nigrostriatal dopaminergic neurons by inhibiting NADPH oxidase and iNOS in the MPTP model of Parkinson's disease. *J Neurol Sci* 348: 142–152; 2015
83. Ross JA, Kasum CM: Dietary flavonoids: bioavailability, metabolic effects, and safety. *Annu Rev Nutr* 22: 19-34; 2002.
84. Roukos V, Pegoraro G, Voss TC, et al: Cell cycle staging of individual cells by fluorescence microscopy. *Nat Protoc* 10: 334-348; 2015
85. Routhier A, Astuccio M, Lahey D, et al: Pharmacological inhibition of Rho-kinase signaling with Y-27632 blocks melanoma tumor growth. *Oncol Rep* 23: 861-867; 2010
86. Sadok A, McCarthy A, Caldwell J, et al: Rho kinase inhibitors block melanoma

- cell migration and inhibit metastasis. *Cancer Res* 75: 2272-2284; 2015
87. Salmani JMM, Zhang XP, Jacob JA, et al: Apigenin's anticancer properties and molecular mechanisms of action: Recent advances and future prospectives. *Chin J Nat Med* 15: 321-329; 2017
88. Schmitz AA, Govek EE, Böttner B, et al: Rho GTPases: Signaling, Migration, and Invasion. *Experimental Cell Research* 261: 1–12; 2000
89. Seregard S, Damato B: Uveal malignant melanoma: management options for brachytherapy. In: Damato B, Singh A (Hrsg.): *Clinical Ophthalmic Oncology*. 173-188, Springer, Berlin, Heidelberg; 2014
90. Shields CL, Shields JA, Perez N, et al: Primary transpupillary thermotherapy for small choroidal melanoma in 256 consecutive cases: outcomes and limitations. *Ophthalmology* 109: 225–234; 2002
91. Shukla S, Gupta S: Apigenin: a promising molecule for cancer prevention. *Pharm Res* 27: 962-978; 2010
92. Singh AD, Turell ME, Topham AK: Uveal melanoma: trends in incidence, treatment, and survival. *Ophthalmology* 118: 1881–1885; 2011
93. Spencer C, Montalvo J, McLaughlin SR, et al: Small molecule inhibition of cytoskeletal dynamics in melanoma tumors results in altered transcriptional expression patterns of key genes involved in tumor initiation and progression. *Cancer Genomics Proteomics* 8: 77–85; 2011
94. Su CC: Tanshinone IIA inhibits human gastric carcinoma AGS cell growth by decreasing BiP, TCTP, Mcl-1 and Bcl-xL and increasing Bax and CHOP

- protein expression. *Int J Mol Med* 34: 1661-1668; 2014
95. Tarmann L, Wackernagel W, Avian A, et al: Ruthenium-106 plaque brachytherapy for uveal melanoma. *Br J Ophthalmol* 99: 1644-1649; 2015
96. Testai L: Flavonoids and mitochondrial pharmacology: a new paradigm for cardioprotection. *Life Sci* 135: 68–76; 2015
97. Torres V, Triozzi P, Eng C, et al: Circulating tumor cells in uveal melanoma. *Future Oncol* 7: 101-109; 2011
98. Tura A, et al: Elevated NG2 expression and Rho-kinase activity in the uveal melanoma cells with monosomy-3. *ARVO Annual Meeting*: 5078:A0023; 2014
99. Van Raamsdonk CD, Griewank KG, Crosby MB, et al: Mutations in GNA11 in uveal melanoma. *N Engl J Med* 363: 2191-2199; 2010
100. Wang JF, Feng JG, Han J, et al: The molecular mechanisms of tanshinone IIA on the apoptosis and arrest of human esophageal carcinoma Cells. *Biomed Res Int* 2014: 582730; 2014
101. Way TD, Kao MC, Lin JK: Degradation of HER2/neu by apigenin induces apoptosis through cytochrome c release and caspase-3 activation in HER2/neu-overexpressing breast cancer cells. *FEBS Lett* 579: 145-152; 2005
102. Wei L, Surma M, Shi S, et al: Novel Insights into the Roles of Rho Kinase in Cancer. *Arch Immunol Ther Exp (Warsz)* 64: 259-278; 2016
103. White VA, Chambers JD, Courtright PD, et al: Correlation of cytogenetic abnormalities with the outcome of patients with uveal melanoma. *Cancer* 83: 354-359; 1998

104. Whitehead J, Tishkovskaya S, O'Connor J, et al: Devising two-stage and multistage phase II studies on systemic adjuvant therapy for uveal melanoma. *Invest Ophthalmol Vis Sci* 53: 4986-4989; 2012
105. Woodman SE: Metastatic uveal melanoma: biology and emerging treatments. *Cancer J* 18: 148-152; 2012
106. Xu S, Liu P: Tanshinone II-A: new perspectives for old remedies. *Expert Opin Ther Pat* 23: 149–153; 2013
107. Yagi A, Takeo S: Anti-inflammatory constituents, aloesin and aloemannan in Aloe species and effects of tanshinon VI in *Salvia miltiorrhiza* on heart. *Yakugaku Zasshi* 123: 517–532; 2003
108. Yamamoto M, Marui N, Sakai T, et al: ADP-ribosylation of the rhoA gene product by botulinum C3 exoenzyme causes Swiss 3T3 cells to accumulate in the G1 phase of the cell cycle. *Oncogene* 8: 1449-1455; 1993
109. Yang J, Manson DK, Marr BP, et al: Treatment of uveal melanoma: where are we now? *Ther Adv Med Oncol* 10: 1758834018757175; 2018
110. Yang X, Zhang Y, Wang S, et al: Effect of fasudil on growth, adhesion, invasion, and migration of 95D lung carcinoma cells in vitro. *Can J Physiol Pharmacol* 88: 874–879; 2010
111. Yu FX, Guan KL: The Hippo pathway: regulators and regulations. *Genes Dev* 27: 355-371; 2013
112. Yu FX, Luo J, Mo JS, et al: Mutant Gq/11 promote uveal melanoma tumorigenesis by activating YAP. *Cancer Cell* 25: 822-830; 2014

113. Yu FX, Zhang K, Guan KL: YAP as oncotarget in uveal melanoma. *Oncoscience* 1: 480–481; 2014
114. Yu J, Wang X, Li Y, et al: Tanshinone IIA suppresses gastric cancer cell proliferation and migration by downregulation of FOXM1. *Oncol Rep* 37: 1394–1400; 2017
115. Yuan SL, Wei YQ, Wang XJ, et al: Growth inhibition and apoptosis induction of tanshinone II-A on human hepatocellular carcinoma cells. *World J Gastroenterol* 10: 2024–2028; 2004
116. Zhou L, Chan WK, Xu N, et al: Tanshinone IIA, an isolated compound from *Salvia miltiorrhiza* Bunge, induces apoptosis in HeLa cells through mitotic arrest. *Life Sci* 83: 394–403; 2008

APPENDIX

1. Abbreviations

µl microliter

µM micrometer

AKT protein kinase B or PKB

AMOT angiomin

AMPK adenosine monophosphate-activated protein kinase

ATP adenosine triphosphate

ATPase adenosine triphosphatase

COMS Collaborative Ocular Melanoma Study

CYP2J2 cytochrome P450 2J2

DAG diacylglycerol

DAPI 4',6-diamidino-2-phenylindol

DNA Deoxyribonucleic acid

dH₂O distilled water

DMEM Dulbecco's modified Eagle's medium

DMSO dimethyl sulfoxide

DNA deoxyribonucleic acid

ECCG epigallocatechin-3-gallate

ECM extracellular matrix

EDTA ethylene diamine tetraacetic acid

EMT epithelial-to-mesenchymal transition

ERK extracellular signal–regulated kinase

ERM ezrin/radixin/moesin

EthD-1 ethidium homodimer-1

F actin filamentous actin

FDA Food and Drug Administration

FBS fetal bovine serum

g gram

G actin globular actin

GAP GTPase activating protein

GEP gene expression profile

GDP guanine diphosphate

GTP guanosine triphosphate

GTPase guanosine triphosphatase

hr(s) hour(s)

HBSS Hanks' balanced salt solution

HCC Hepatocellular carcinoma

IC₅₀ 50% inhibiting concentration

IgG immunoglobulin

IP₃ inositol 1,4,5-trisphosphate

LASTS large tumor suppressor homologue

M mole

MAPK mitogen-activated protein kinase

MBS phosphorylate myosin-binding subunit

MEK mitogen-activated protein kinase kinase or MAPKK

mg milligram

MLC myosin light chain

mM millimolar

MST mammalian STE20-like protein kinase

mTOR mammalian target of rapamycin

MTT 3-(4, 5-dimethylthiazolyl)-2, 5 diphenyl tetrazolium bromide

MW Molecular weight

MYPT1 myosin phosphatase target subunit-1

NEBD nuclear envelope breakdown

NHE1 Na⁺/H⁺ exchange protein

P-MYPT1 phospho-myosin phosphatase target subunit-1

PBS phosphate buffered saline

PCA polycyanoacrylate

PDT photodynamic therapy

PFA paraformaldehyde

PI3K phosphatidylinositol-3 kinase

PKC protein kinase C

PLC-β phospholipase C-β

QNA11 guanine nucleotide-binding protein subunit alpha-11

QNAQ guanine nucleotide-binding protein subunit alpha-Q

Rho ras-homology

ROCK Rho-associated coiled-coil kinase/ROK

RPE retinal pigment epithelium

SEM standard error of mean

SEM scanning electron microscopy

S-phase synthesis phase

TTT transpupillary thermal therapy

UM uveal melanoma

UMM uveal melanoma medium

UV ultraviolet

VEGF vascular endothelial growth factor

YAP yes-associated protein

TAN IIA tanshinione IIA

2. Materials

- Alexa488-phalloidin, Thermo Fisher scientific, # A12379
- Alexa Fluor 488 conjugated goat anti-rabbit IgGs, Abcam, # ab150077
- (Rabbit) Anti-Ki67 antibody, Abcam, # ab15580
- (Rabbit) Anti-MYPT1, Abcam, # ab32519
- (Rabbit) Anti-phospho T696-MYPT1, Abcam, # ab59202
- (Rabbit) Anti-YAP1, Abcam, # ab52771
- Apigenin, Sigma-Aldrich, # A3145
- DAPI, Invitrogen, # D1306
- Dimethyl sulfoxide (DMSO), Carl Roth, # 4720.1
- Ethanol, Carl Roth, # 9065.2
- Ethylene diamine tetraacetic acid (EDTA), ROTH, # 8043.2
- Ethidium homodimer-1(EthD-1), Thermo Fisher Scientific, # E1169
- Fetal bovine serum, gibco, life technologie, # 10100-147
- Hanks' balanced salt solution (HBSS), gibco, life technologies, #14170-088
- KCl, Merck Millipore, #1.04936.0500
- KH_2PO_4 , Fluka, # R00125
- Mowiol, Carl Roth, # 07132
- Na_2HPO_4 , Merck Millipore, # 1.06586.0500
- NaCl, J.T.Baker, # 1764
- Tanshinone IIA, Enzo life sciences, # GR-336-0005
- Tris-HCl, Carl Roth, # 9090.1

- Triton X-100, Serva, # 39795
- Paraformaldehyde, Merck Millipore, # 1.04005.1000
- Penicillin/Streptomycin, Biochrom, # A2212
- Phosphate buffered saline (PBS), without Ca⁺⁺ and Mg⁺⁺, for cell culture, Merck Millipore, # L1825
- RPMI-1640 with 2mM L-Glutamine, Lonza, # BE12-752F
- 1×Trypsin-EDTA (0.25% Trypsin with 1mM EDTA, without Ca⁺ and Mg²⁺), Merck Millipore, # L2143
- 3% Bovine serum albumin, Sigma, # A4303

2. Laboratory containers, glasswares, and other materials

- 8-well chamber slide, Sarstedt, # 94.6140.802
- 12-well chamber slide, ibidi, # 81201
- 24-well plate, Greiner Bio-One, # 662160
- 24 x 60 mm coverslip, Menzel, # CS2460100
- 75 cm² culture flask, Greiner Bio-One, # 658175
- 96-well cell culture plate, Sarstedt, # 83.3924
- Millex GS 0.22 µm filter unit, Millipore, Billerica, MA, # SLGSO33SS

3. Laboratory apparatus and computer softwares

- Autoclave, Systec, # DX-23
- Centrifuge, Sigma, # 2-16PR
- Colorimeter, FLUOstar OPTIMA microplate reader, # 413-2002

- Cytometer with Neubauer chamber, Heinz Herenz Medizinalbedarf GmbH, Germany
- Fluorescence microscopy, Leica DMI 6000 B microscope, Wetzlar, Germany
- Fluorescence monochrome digital camera, DFC 350 FX, Leica Microsystems.
- Filter sets, indicated by *Table 3*
- **Fiji is Just ImageJ (Fiji)** program, National Institutes of Health, USA, <https://imagej.net/Fiji/Downloads>, 2007–2017
- Incubator, Sanyo, # MCO-17A1
- Leica application suite software, Advanced Fluorescence 2.7.0
- Leica application suite software, V3.7 (build 871), 2003-2010 (scratch assay)
- Microscope for scratch assay, Leica DFC295
- Microsoft Excel software for Mac 2011, 14.7.2 (170228), 2010 Microsoft Corporation, U.S
- MTT phase contrast microscope, Leica DFC295, Germany
- Water bath, GFL, #1083

4. Buffers and solutions

Apigenin stock solution

Under a laminar flow hood, apigenin (Molecular weight: 270.24) was dissolved in sterile DMSO at a final concentration of 50 mM, aliquotted into sterile 500 µl microtubes wrapped in aluminum foil, and stored at -20°C protected from light.

DAPI stock solution (1µg/ml)

20 µl of DAPI (5 mg/ml) was dissolved in 100 ml 1×PBS on a magnetic stirrer for one hour under protection from light, aliquotted into 50 ml tubes wrapped in aluminum foil, and stored at 4°C.

Blocking buffer

- 120 mM KCl
- 20 mM NaCl
- 5 mM EDTA
- 10 mM Tris-HCL, pH 7.5
- 3% Bovine serum albumin
- dH₂O

Dissolved in 160 ml dH₂O to reach the final volume 200 ml. The solution was sterile filtered with 0.22 µm filters and stored at 4°C.

Mowiol

- 6.4 g Mowiol 4-88
- 16 g Glycerol
- 32 ml 0.2M Tris-HCL

6.4 mg Mowiol and 16 g Glycerol was mixed and stirred for one hour under room temperature. Afterwards, 16 ml of aqua tridest was added and the mixture was stirred for one hour under room temperature. 32 ml Tris-HCL was added and the stirring was continued for 2 hours at 50°C, followed by an overnight stirring at room

temperature. On the next day, the solution was centrifuged at 5000 rpm for 15 minutes to precipitate the undissolved Mowiol. The supernatant was aliquotted at ca. 1.5 ml and stored at -20°C.

MTT stock solution (5 mg/ml)

- 0.25 g MTT
- 50ml PBS (cell culture grade, without Ca⁺⁺ and Mg⁺⁺)

MTT pulver was dissolved in PBS by rotating overnight protected from light. The solution was sterile filtered using 0.22 µm filters and stored at 4°C.

Tanshinone IIA stock solution

Under a laminar flow hood, tanshinone IIA (MW: 294.3) was dissolved in sterile DMSO at a final concentration of 50 mM, aliquotted into sterile 500 µl microtubes wrapped in aluminum foil, and stored at -20°C protected from light.

4% paraformaldehyde

- 4 g paraformaldehyde
- 100 ml PBS

Stirred under fume hood and heated to approximately 60°C until the solution appeared clear. Stored at 4°C.

10X PBS

- 80 g NaCl (MW=58,44)
- 2.7 g KCl (MW=74.55)
- 11.5 g Na₂HPO₄ (MW=141.96; anhydrous)
- 2 g KH₂PO₄ (MW=139.09)

Adjusted the volume of 10X PBS to 1 liter 1X PBS using dH₂O. Stored at room temperature.

ACKNOWLEDGEMENT

I am very grateful to Prof. Salvatore Grisanti for providing me this precious opportunity to conduct this novel project. I would like to express my deepest appreciation for his valuable and constructive suggestions and friendly support throughout my entire work.

I would like to thank Dr. Aysegül Tura for not only the inspiring idea and brilliant design of this project, but also for her patience and continuous motivation throughout every step of my work.

I also express my thanks to Mrs. Christine Örun for her friendly support in the laboratory.

I should not forget to mention my gratitude to Mrs. Petra Hammermeister for her immeasurable support during my difficult times.

I am also grateful to my colleagues at the Labor for the pleasant working atmosphere.

My particular gratitude goes to my country and the Chinese Scholarship Council (CSC). Without the significant financial support I couldn't finish my doctoral work in Germany.

Finally I would like to thank all the members of my family for their endless support.

Disclosure: H Zuo received financial support from the China Scholarship Council (grant number: 201608080102).

CURRICULUM VITAE

Huaxin Zuo



PERSONAL DATA

Birth date	22. March 1988
Birth place	Heilongjiang, China
Nationality	Chinese
Address	Maria-Goeppert-Str.18 23562 Lübeck
Tel.-Nr.	+49 (0)15166073976
Email	zuohuaxin@163.com

EDUCATION

10/2015 - now	Doctoral dissertation <i>Universität zu Lübeck, Lübeck, Germany</i>
09/2012 - 07/2015	Master of Ophthalmology <i>Capital Medical University, Beijing, China</i>
09/2007 - 06/2012	Bachelor of Clinical Medicine <i>Harbin Medical University, Harbin, China</i>

CERTIFICATION

12/2014	Medical licence <i>Certificated in Beijing, China</i>
---------	--

TRAINING

10/2015 - now	Doctoral student <i>Labor of the Ophthalmology Clinic of the UKSH</i>
09/2012 - 07/2015	Ophthalmology Resident <i>Beijing TONGREN Hospital, Beijing, China</i>
07/2011 - 06/2012	Intern

PRESENTATIONS IN CONFERENCES

10/2017	115. Kongress der Deutsch Ophthalmologische Gesellschaft (<i>Berlin, Germany</i>)
06/2017	67. Tagung der Vereinigung Norddeutscher Augenärzte (<i>Sylt, Germany</i>)

PUBLICATIONS

Zuo H, Grisanti S and Tura A. The flavonoids Tanshinone IIa and Apigenin as potential and natural inhibitors of the metastatic activities of uveal melanoma cells. DOG 2017 Annual Meeting, Berlin Germany, 2017, Presentation abstract, PSa07-06.

Zuo H, Wang T and Wang H. Treatment progress of Anti-VEGF therapies for neovascular glaucoma. International Review of Ophthalmology. 2014, 38 (6): 425-428. DOI: 10.3760/ cma. j. issn.1673-5803.2014.06.014.

Wang H, Wang T, Zhang F and **Zuo H**. Management of neovascular glaucoma with intravitreal Ranibizumab and subsequent trabeculectomy with mitomycin C combined with panretinal photocoagulation. Chinese journal of practical Ophthalmology. 2015, 33(4): 370-373. DOI: 10.3760/cma.j.issn.1006-4443.2015.04.011.